THE ASTROPHYSICAL JOURNAL SUPPLEMENT SERIES, 99:349–389, 1995 August

VLA MAPS OF RADIO GALAXIES TO $z = 1$

S. G. NEFF,[1] L. ROBERTS,[2] AND J. B. HUTCHINGS[3]
Received 1994 August 17; accepted 1994 December 6

ABSTRACT

We present 6 and 20 cm maps of a sample of 49 radio galaxies with $z \sim 0.1$–1.0. The sources were chosen without knowledge of morphology and spectral index, to match as nearly as possible the 11 cm flux/redshift distribution of a previously observed sample of quasars (Price et al. 1993). The observations were made with the VLA[4] in its A configuration, to match those of the quasar sample. The properties of these sources have been discussed and compared with the quasars in Hutchings et al. (1994). In this paper we also give the source flux measures and comments on the correspondence with the optically imaged host galaxies.

Subject headings: galaxies: structure — radio continuum: galaxies — surveys

1. INTRODUCTION AND OBSERVATIONS

In a series of papers (Hutchings, Price, & Gower 1988b, hereafter HPG; Neff, Hutchings, & Gower 1989; Neff & Hutchings 1990), we studied the radio morphology of ~250 quasars, using VLA A-configuration observations. The maps to redshift 1 are published in Price et al. (1993) and Gower & Hutchings (1984). In that work, we selected samples to fill the redshift-luminosity plane as widely and evenly as possible, with no preknowledge of morphology or spectral index, in order to make an unbiased study of radio morphologies. The present paper presents the data from a parallel investigation of the radio structures of radio galaxies. We obtained maps of a sample of 49 objects classified by others as radio galaxies in the redshift interval 0.1–1.0. The sample was selected to match the $z < 1$ HPG quasar sample as closely as possible in the redshift-luminosity plane. Discussion of the radio galaxy properties and their relationship with the quasars is given in Hutchings et al. (1994).

The observations were made on 1987 October 3, 10, and 11. Snapshot VLA observations were made in A array at 6 and 20 cm (4848 and 1478 MHz, respectively, with total bandwidths of 50 MHz). Most sources were observed at both wavelengths; in a few cases 20 cm A-array maps were published in the literature, so we did not reobserve those sources. Observations were typically 5 minutes at each wavelength, providing a good match in sensitivity to the HPG quasar sample. The data were calibrated using 3C 286 (assumed total flux densities of 7.45 Jy at 4848 MHz and 14.45 Jy at 1478 MHz) and 3C 48 (assumed total flux densities of 5.40 Jy at 4848 MHz and 15.27 Jy at 1478 MHz). The Astronomical Image Processing System (AIPS) was used to produce (uniform weighted, tapered, and full-resolution) maps of the radio intensity; the images were CLEANed and in most cases self-calibrated (phase only). Our detection limits range from less than 0.5 to 1.0 mJy at 6 cm, and from 0.6 to 1.0 mJy at 20 cm. AIPS was also used to measure the fluxes reported here.

2. MEASUREMENTS

Table 1 of Hutchings et al. (1994) gives a summary of source morphologies and fluxes, as well as other properties. In this paper, we give the source component fluxes and map centers in Table 1. The "core" fluxes given are the peak fluxes found in the untapered maps at or near the optical galaxy positions. This "core" flux is typically the response of a point source to a ~0".4 (6 cm) or ~1".4 (20 cm) (FWHM) Gaussian beam. The "lobe" fluxes given are integrated fluxes measured in tapered maps with Gaussian beams of FWHM ~ 0".8 (6 cm) or ~3" (20 cm) and should be regarded as lower limits to the extended flux present in the sources. Measurements were performed on CLEANed and also tapered maps, and in general these agreed to a few percent. The values quoted are averages except where one or other was clearly more reliable.

In Hutchings et al. (1994) we also discussed a second group of radio galaxies called the Weadock sample. These galaxies were selected differently from those reported here and observed with different VLA configurations. Details of those maps will be published elsewhere by McHardy and collaborators.

The maps are shown in Figure 1. Table 2 lists all the contour levels used and other data relevant to the maps.

3. INDIVIDUAL SOURCES

In this section we give comments on individual sources, arising from our radio maps, our own optical images, or other published information. Optical images of several of the galaxies are published in Hutchings, Johnson, & Pyke (1988a). Several of the sources have been the subject of more detailed investigations, but we have not attempted to list them here.

3C 6.1.—This source has two bright hot spots and faint inner lobe structure that suggests a changing orientation of the (undetected) core.

54W067, 54W068, 54W084.—These sources were included in order to cover lower luminosity objects in the sample. Un-

[1] Laboratory for Astronomy and Solar Physics, Code 681, Goddard Space Flight Center, Greenbelt, MD 20771.

[2] Hughes/STX, Code 681, Goddard Space Flight Center, Greenbelt, MD 20771.

[3] Dominion Astrophysical Observatory, 5071 West Saanich Road, Victoria, BC V8X 4M6, Canada.

[4] The Very Large Array is a part of the National Radio Astronomy Observatory, which is operated by Associated Universities, Inc., under contract with the National Science Foundation.

TABLE 1

RADIO GALAXIES STUDIED AND THEIR PROPERTIES

Name		m	z	Map center (1950) H M S	° m s	6cm flux (mJy) C	L1	L2	20cm flux (mJy) C	L1	L2
4C6.1	0013+790	22.0	0.84	00 13 34.4	79 00 10	4.4	520	563	0	1520	1738
54W067	0015+163	–	–	00 15 34.9	16 20 53	-	-	-	19	183	
54W068	0015+165	–	–	00 15 35.0	16 32 53	3.3	0	0	0	66	314
54W084	0016+157	–	0.54	00 16 06.2	15 45 30	0	0	0	0	1	3
OB343	0026+346	20.4	0.60	00 26 34.8	34 39 58	1225	0	0	1857	0	0
3C34	0107+315	20.5	0.69	01 07 32.5	31 31 22	0	95	111	0	537	753
3C41	0123+329	21.0	0.79	01 23 54.7	32 57 39	0	383	751	0	1457	2255
3C46	0132+376	19.5	0.44	01 32 34.1	37 38 47	3.6	0	11	11	390	376
3C49	0138+136	21.0	0.62	01 38 28.5	13 38 20	733	161	0	2600	0	0
4C61.1	0211+861	19.0	0.18	02 10 45.2	86 05 08	0	118	337	0	857	1520
4C05.16	0347+057	20.9	0.76	03 47 07.0	05 42 35	0	724	410	0	2130	1030
3C99	0358+005	19.1	0.43	03 58 33.3	00 28 11	200	290	19	1538	0	0
3C105	0404+036	18.5	0.09	04 04 48.1	03 32 50	1126	0	0	3464	0	0
4C74.08	0407+747	20.5	0.63	04 07 06.0	74 43 24	0	148	374	0	1088	1786
3C123	0433+296	21.7	0.22	04 33 55.3	29 34 19	0	10	5900	0	27300	33140
3C132	0453+227	18.5	0.21	04 53 42.0	22 44 43	0	365	569	0	1290	2031
OG3	0500+020	21.4	1.00	05 00 45.2	01 58 54	1920	0	0	2204	0	0
3C153	0605+481	18.5	0.28	06 05 44.6	48 04 49	0	690	644	0	2210	1673
3C166	0642+214	19.5	0.25	06 42 24.7	21 25 03	610	0	61	464	520	1105
3C169.1	0647+452	20.5	0.63	06 47 35.5	45 13 01	0	0	138	0	427	671
3C171	0651+542	18.8	0.24	06 51 11.0	54 12 50	0	464	398	0	1811	1698
OI417	0710+439	19.9	0.52	07 10 03.3	43 54 26	1548	0	0	1930	0	0
3C175.1	0711+147	21.5	0.92	07 11 14.3	14 41 34	11	289	200	0	1100	691
3C187	0742+021	19.5	0.35	07 42 27.9	02 07 44	3	44	26	4	463	459
–	0801+364	–	0.51	08 01 48.4	36 27 45	0	51	15	0	0	0
3C195	0806–103	17.8	0.18	08 06 29.9	-10 19 10	28	51	121	66	896	1512
3C196.1	0812–030	17.5	0.20	08 12 57.3	-02 59 14	126	330	0	750	1050	0
3C197.1	0818+472	16.5	0.13	08 18 00.9	47 12 11	7	100	165	0	926	762
4C55.16	0831+557	17.5	0.24	08 31 04.4	55 44 41	5276	0	0	7937	0	0
–	0835+373	–	0.49	08 35 11.8	37 21 07	144	0	0	0	0	0
–	0850+342	–	0.90	08 50 35.2	34 17 44	0	157	66	0	0	0
3C219	0917+458	17.2	0.17	09 17 50.7	45 51 44	44	43	0	61	1662	643
3C223	0936+361	17.1	0.14	09 36 50.9	36 07 35	4.3	0	0	0	0	0
3C234	0958+290	17.3	0.19	09 58 57.4	29 01 37	47	559	321	62	2693	1150
3C236	1003+351	16.0	0.10	10 03 05.4	35 08 48	900	400	0	3135	0	0
3C244.1	1030+585	19.0	0.43	10 30 19.5	58 30 06	0	418	282	0	1750	1750
3C258	1122+196	19.5	0.17	11 22 06.4	19 35 59	383	0	0	845	0	0
–	1125+325	–	0.95	11 25 31.0	32 32 23	0	123	75	0	0	0
3C263.1	1140+224	20.0	0.37	11 40 49.2	22 23 35	2.8	308	464	0	1502	1295
3C268.2	1158+318	19.3	0.36	11 58 24.8	31 50 02	0	25	62	0	561	621
3C268.3	1203+645	20.0	0.37	12 03 54.1	64 30 18	730	408	0	2805	1210	0
–	1253+292	23	–	12 53 44.0	29 10 37	61	0	0	136	0	0
–	1255+298	22.5	–	12 55 29.2	29 49 45	7	0	0	0	9	20
–	1256+286	22.5	–	12 56 29.5	28 34 03	0	5	0	0	61	47
3C411	2019+098	19.7	0.47	20 19 44.2	09 51 34	97	300	450	64	1310	1756
OW637	2021+615	19.5	0.23	20 21 13.3	61 27 18	1527	0	0	1993	0	0
3C427.1	2104+763	21.0	0.57	21 04 45.0	76 21 10	0	477	632	0	1390	1981
3C435	2126+073	21.0	0.47	21 26 37.0	07 19 46	17	88	142	9	417	580
3C441	2203+292	22.0	0.71	22 03 49.5	29 14 46	0	644	361	0	1702	670
3C462	2324+405	20.5	0.63	23 24 30.6	40 31 39	0	672	331	26	1549	903
4C45.51	2351+456	20.6	0.66	23 51 50.0	45 36 23	1218	0	0	1976	0	0
OZ488	2352+495	19.0	0.24	23 52 37.8	49 33 27	1410	0	0	2341	0	0

fortunately the optical identifications and redshifts are not well established, and there is some uncertainty as to whether the sources are single or multiple (R. A. Windhorst 1994, private communication). Kron, Koo, & Windhorst (1987) give some optical and radio details.

3C 34.—This is a large source with much detailed structure in the lobes in our 6 cm map.

3C 41.—This source has two bright hot spots at the lobe ends, and the faint structure, like 3C 6.1, suggests changing orientation of the central engine, but no detected core.

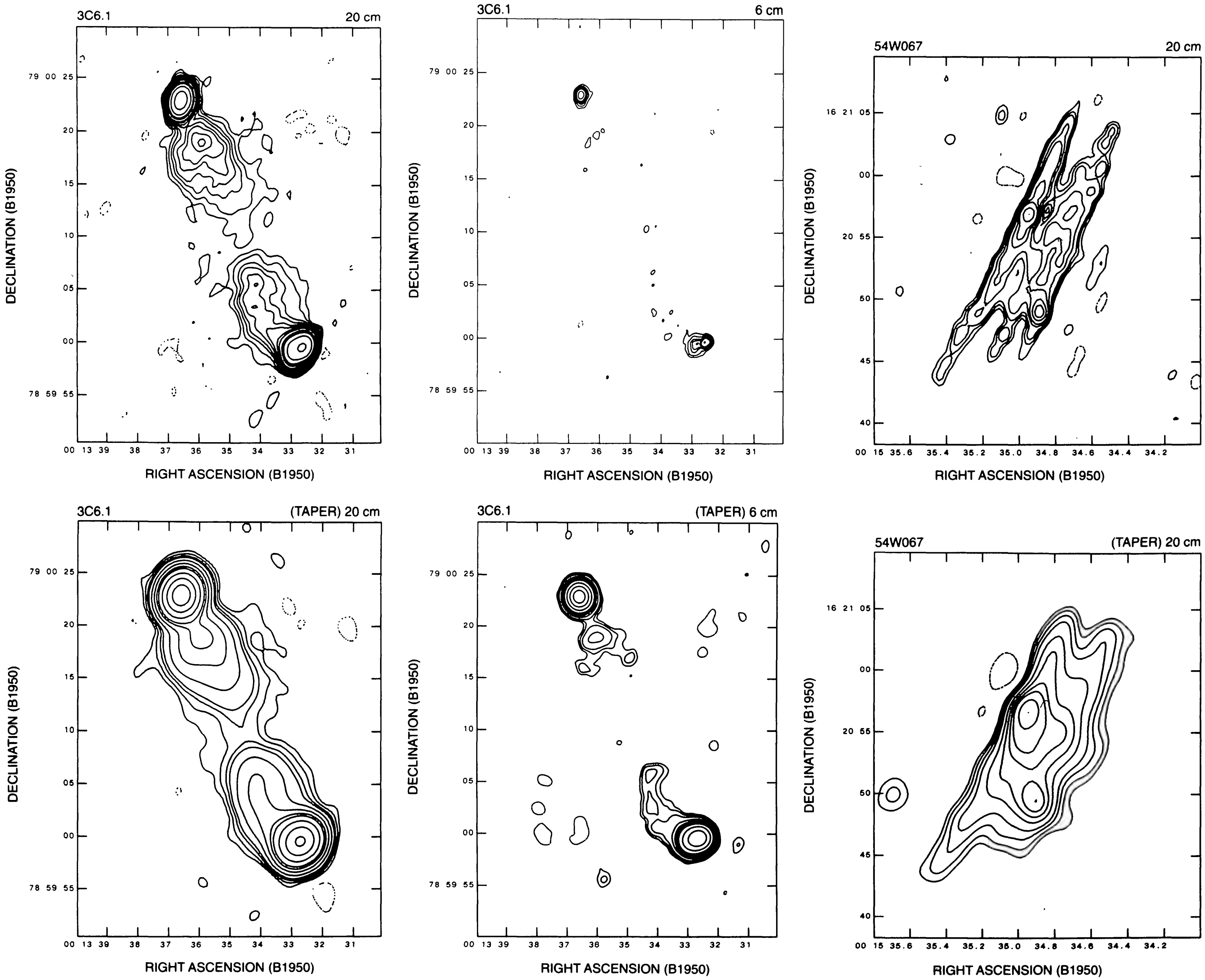

FIG. 1.—Contour maps of the sources as labeled. The contour levels are given in Table 2. Table 1 summarizes the flux measures and gives the map centers.

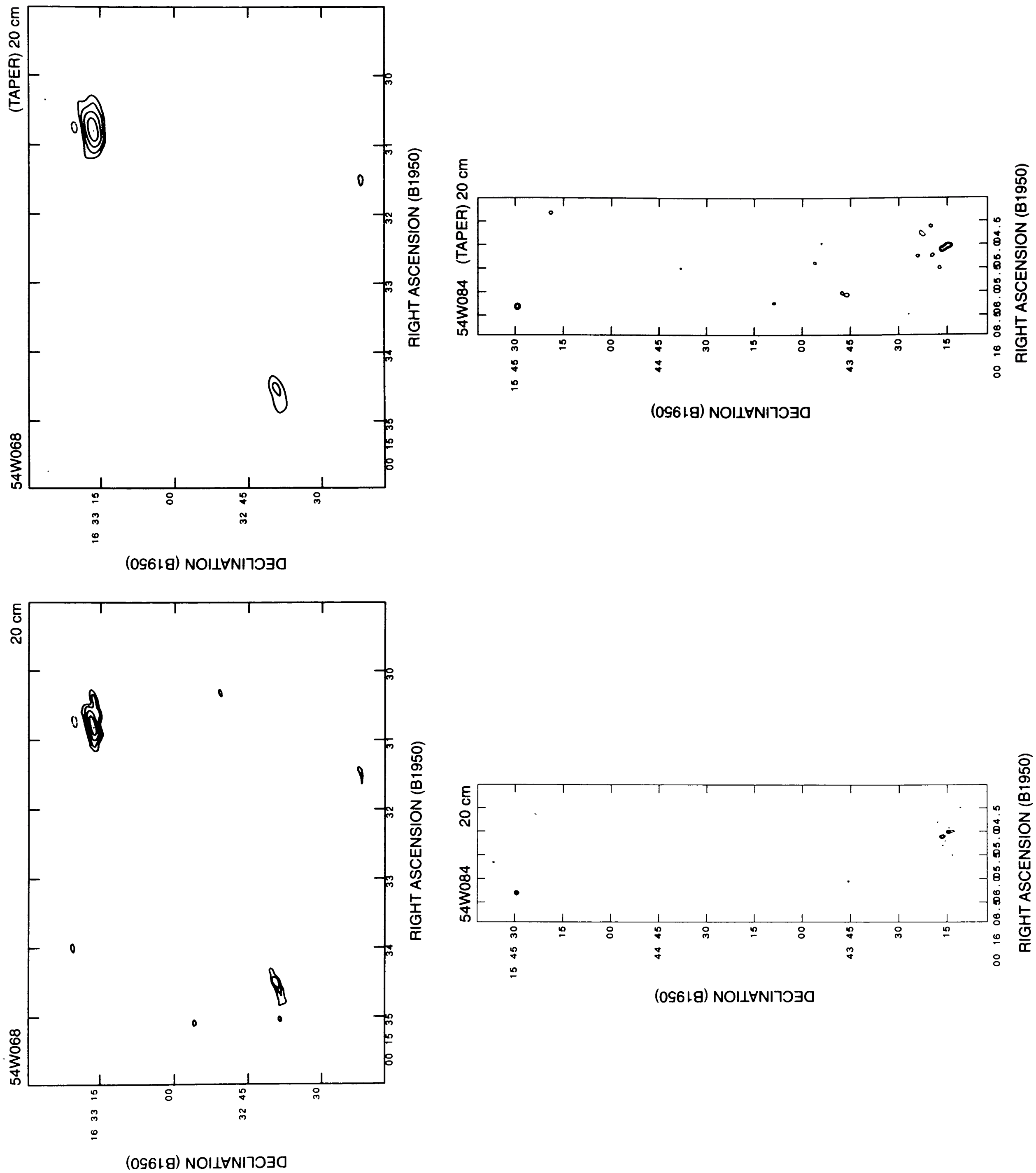

FIG. 1—*Continued*

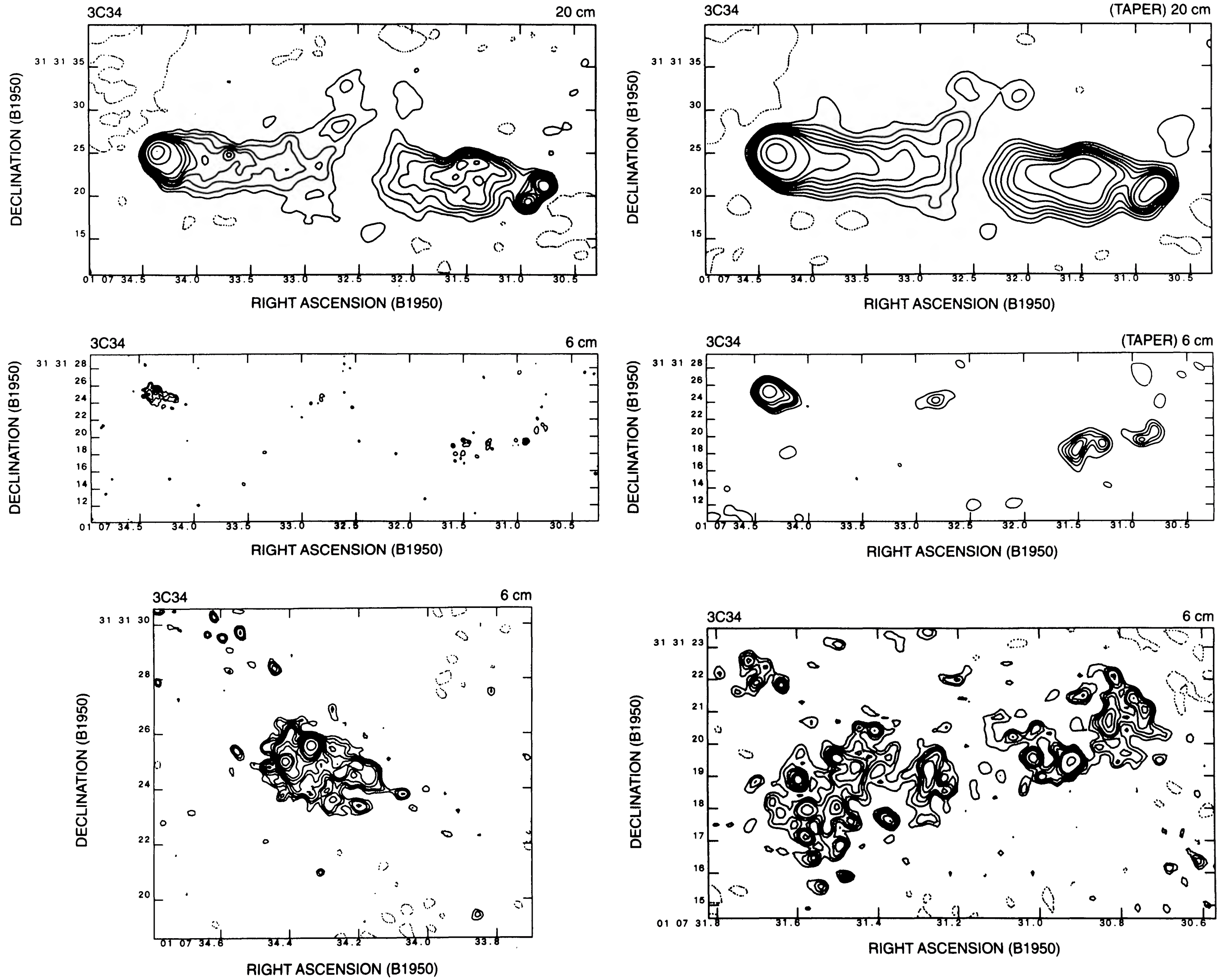

FIG. 1—*Continued*

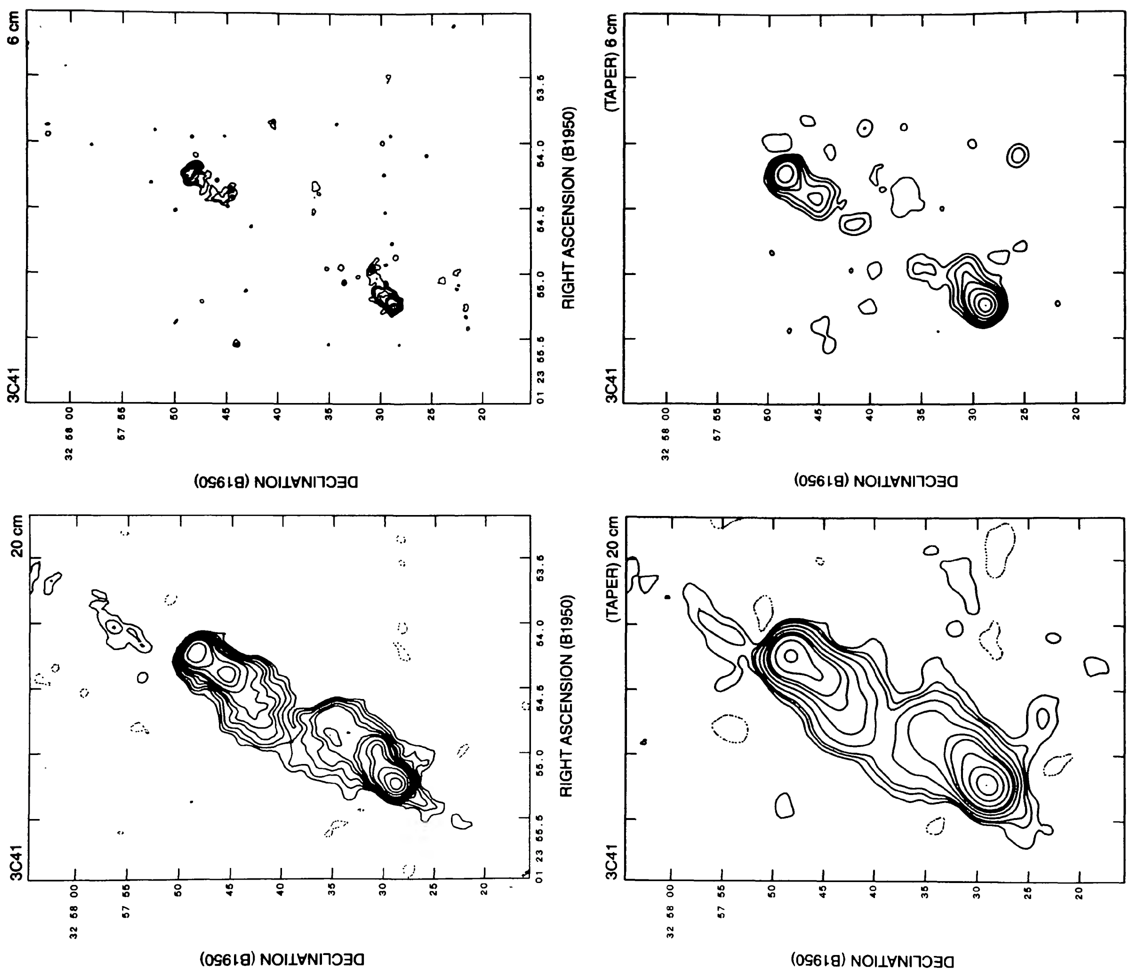

FIG. 1—*Continued*

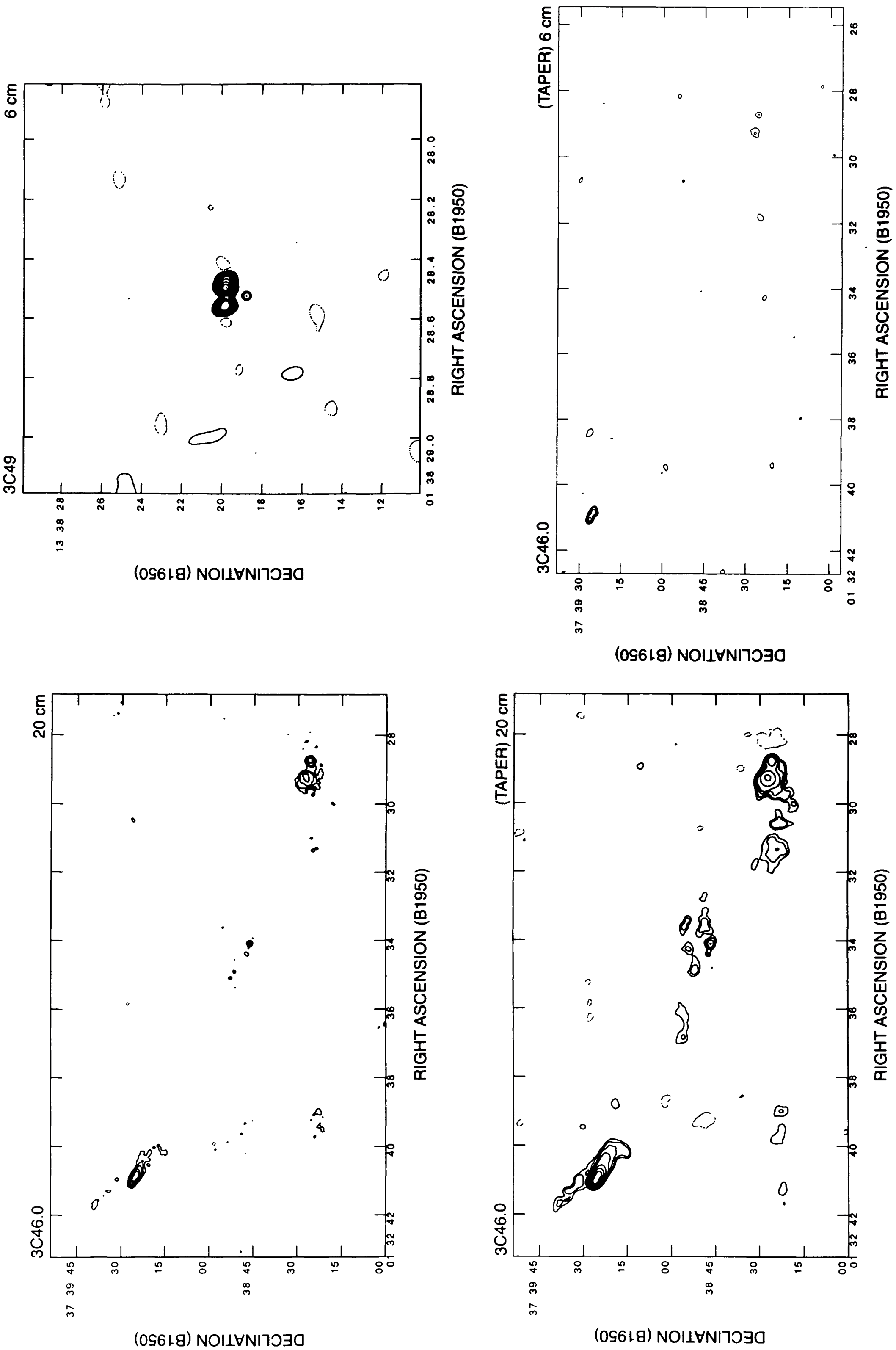

FIG. 1—*Continued*

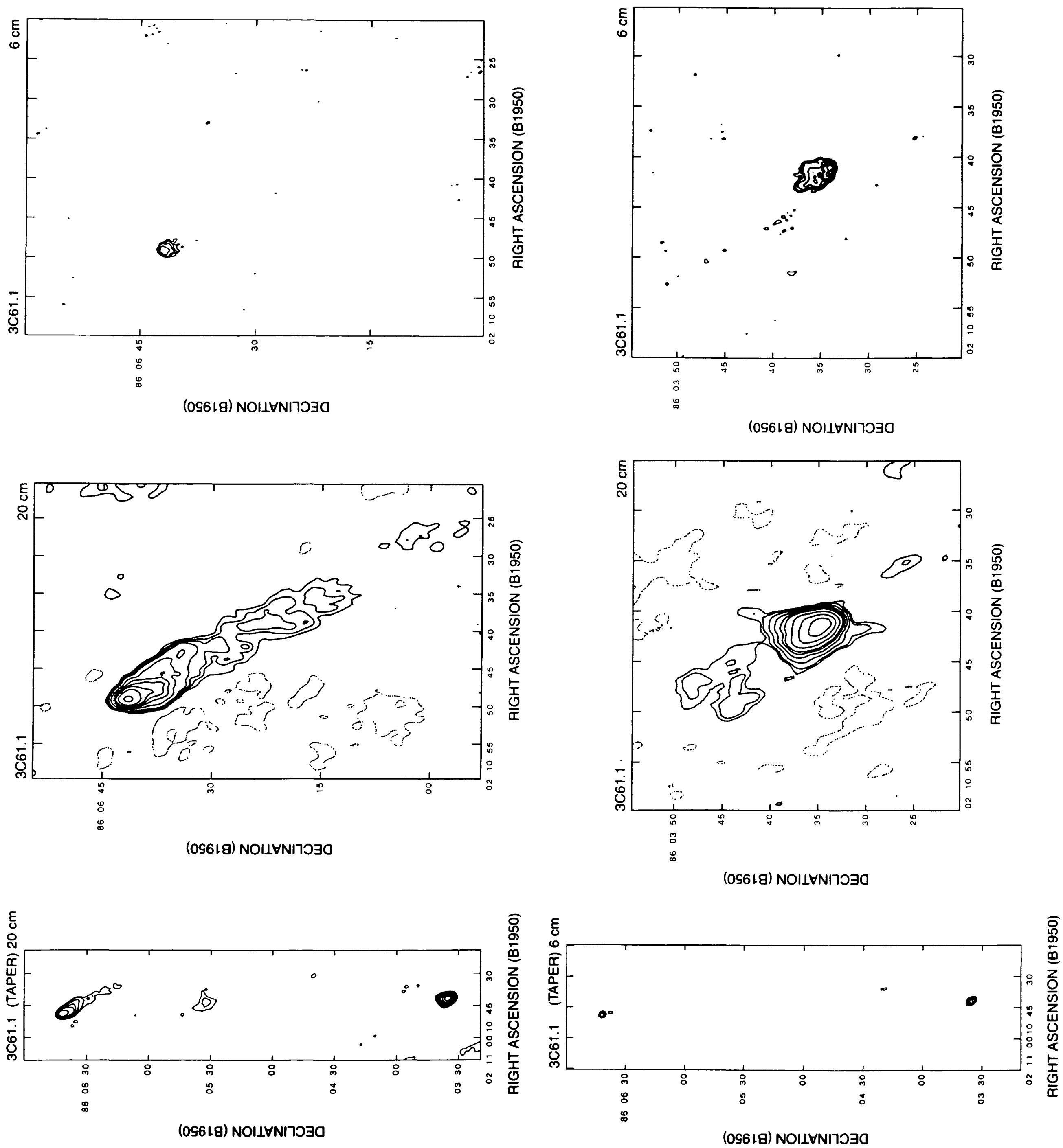

FIG. 1—*Continued*

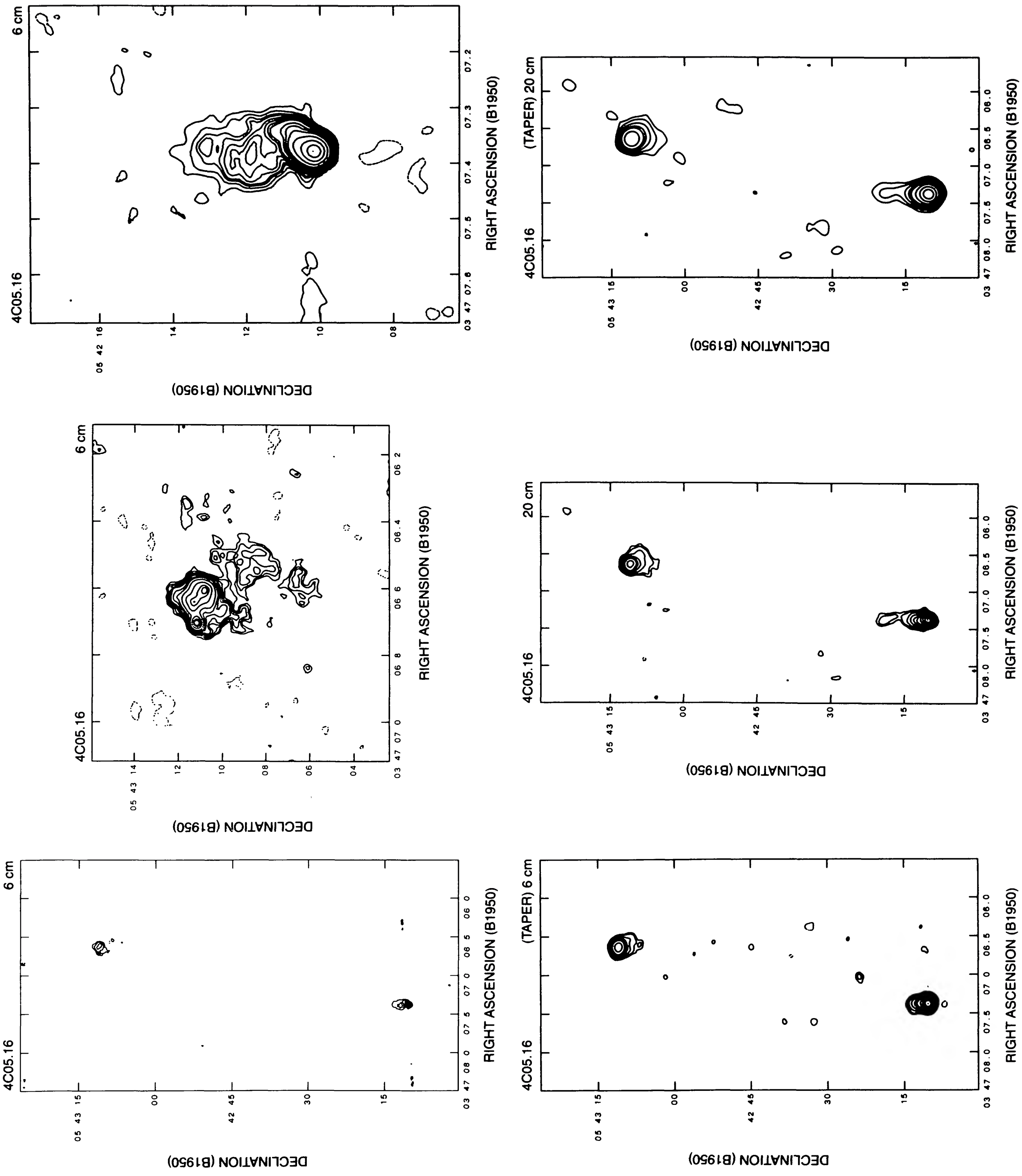

FIG. 1—*Continued*

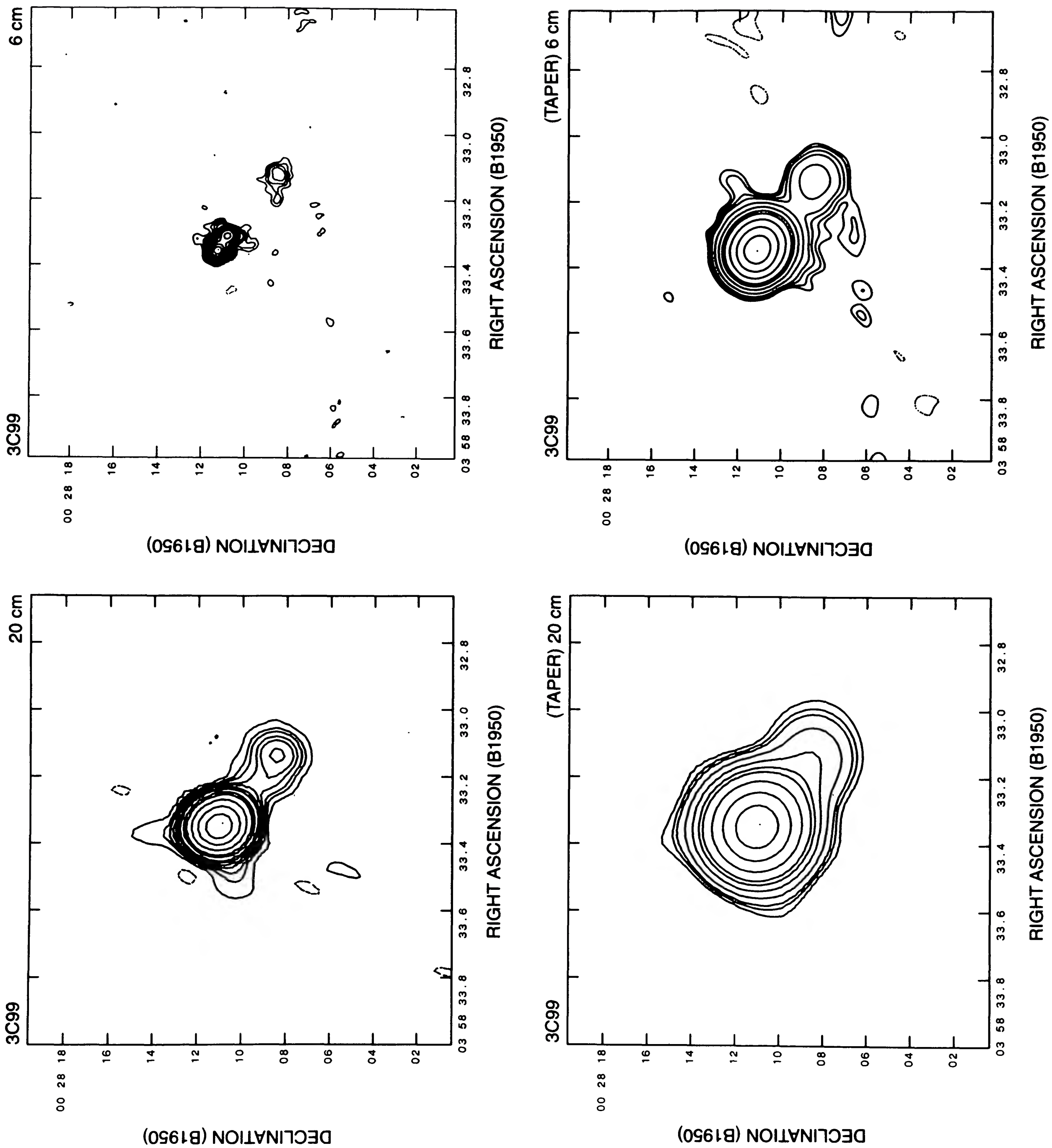

FIG. 1—*Continued*

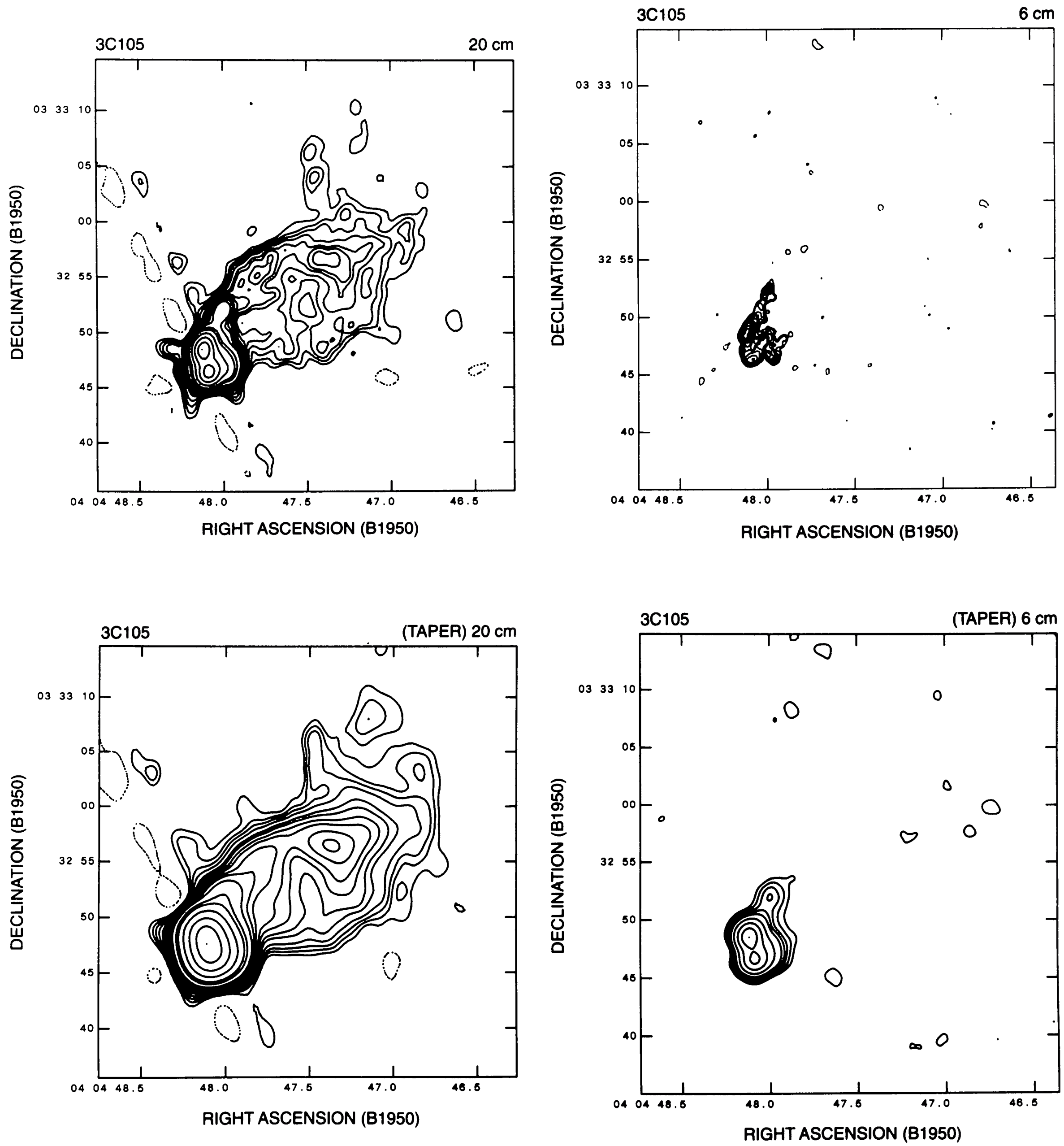

FIG. 1—*Continued*

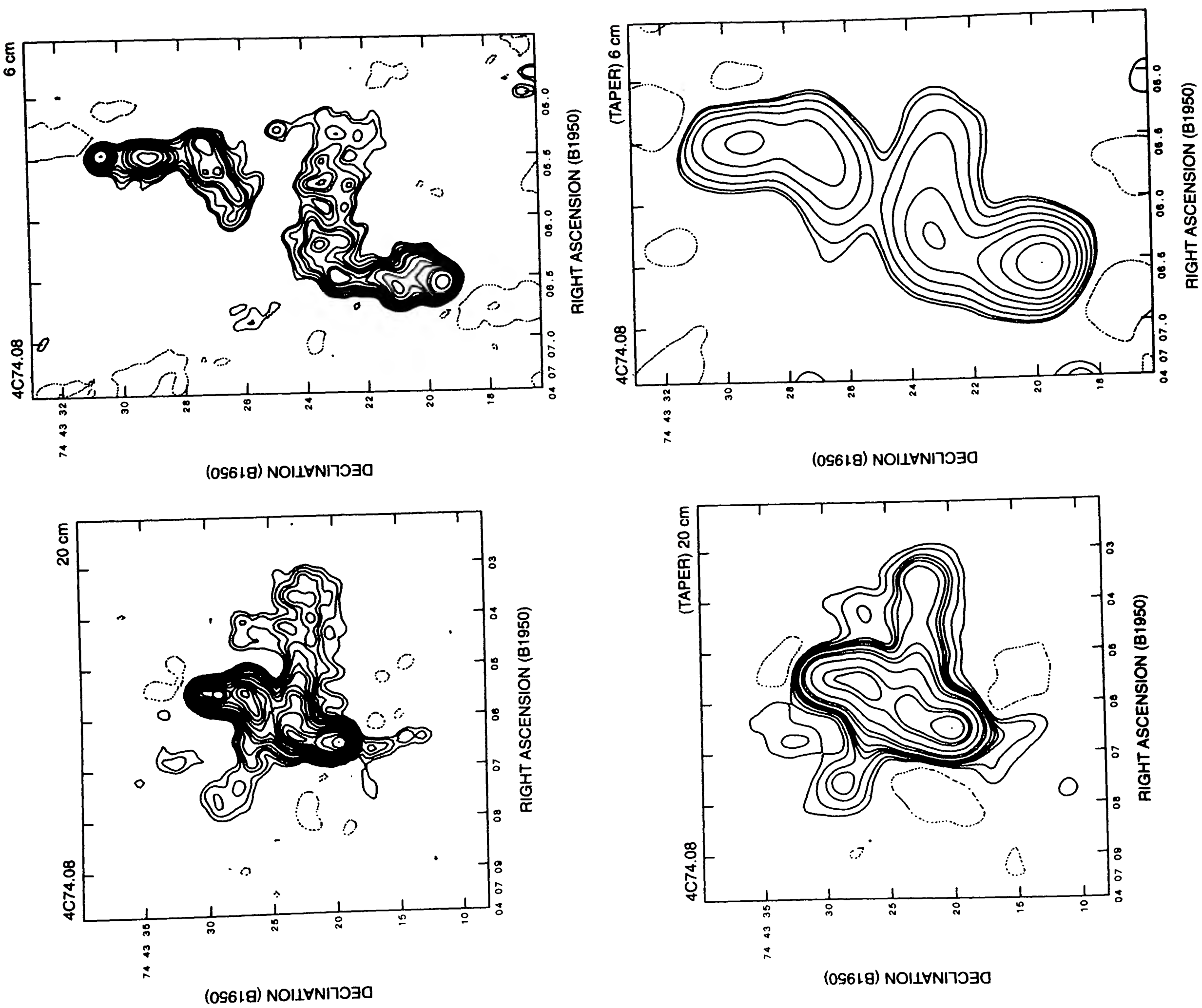

FIG. 1—*Continued*

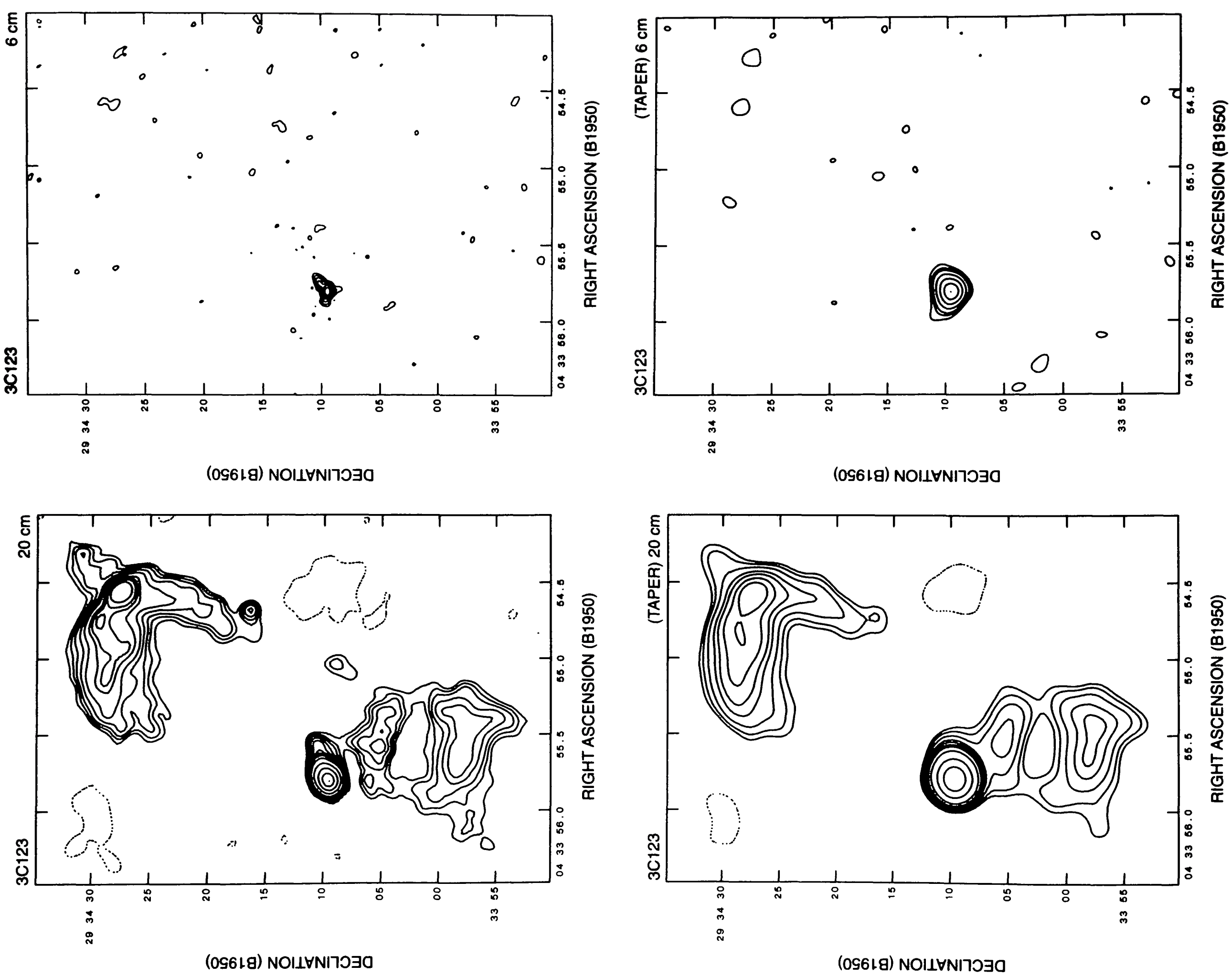

FIG. 1—*Continued*

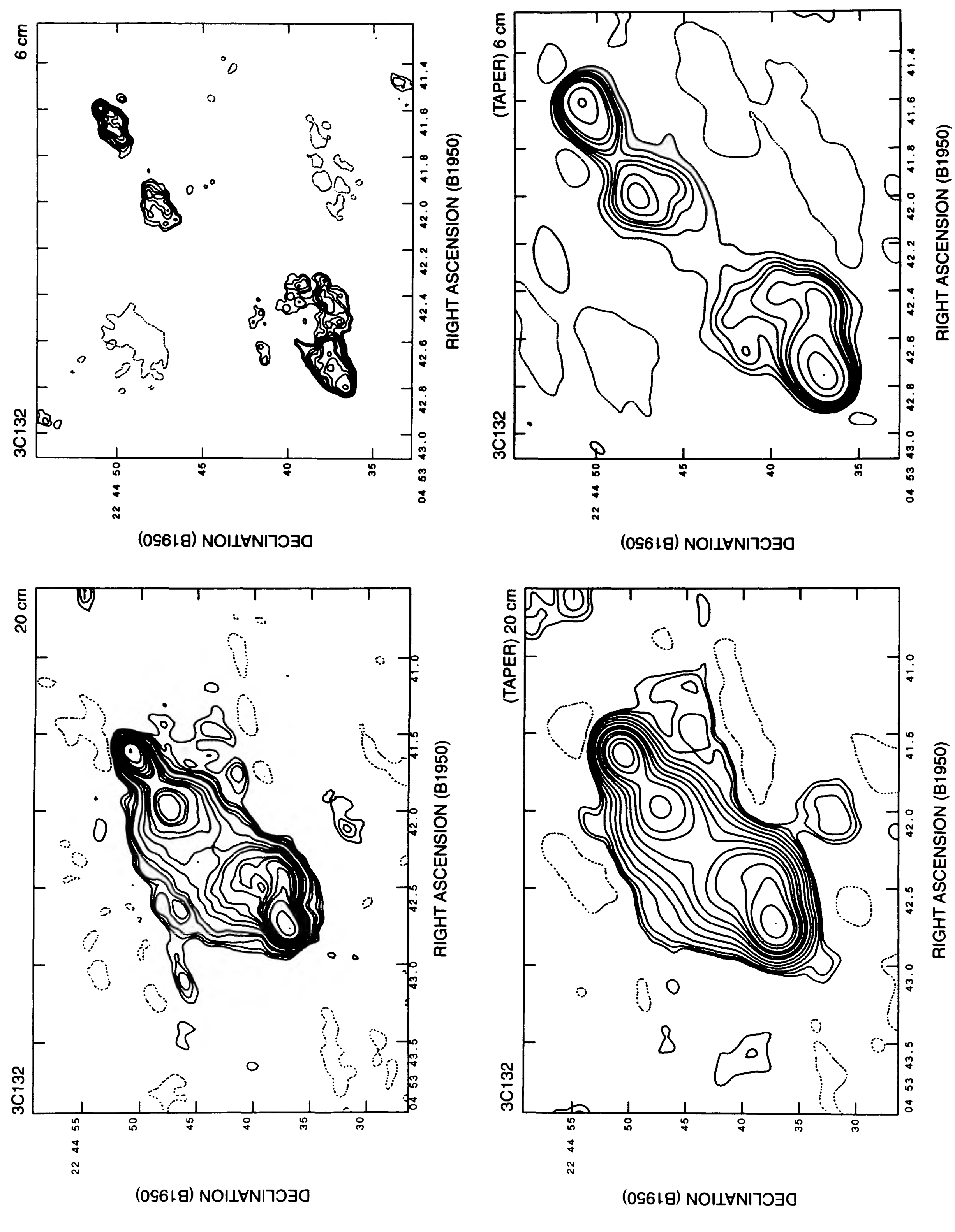

Fig. 1—*Continued*

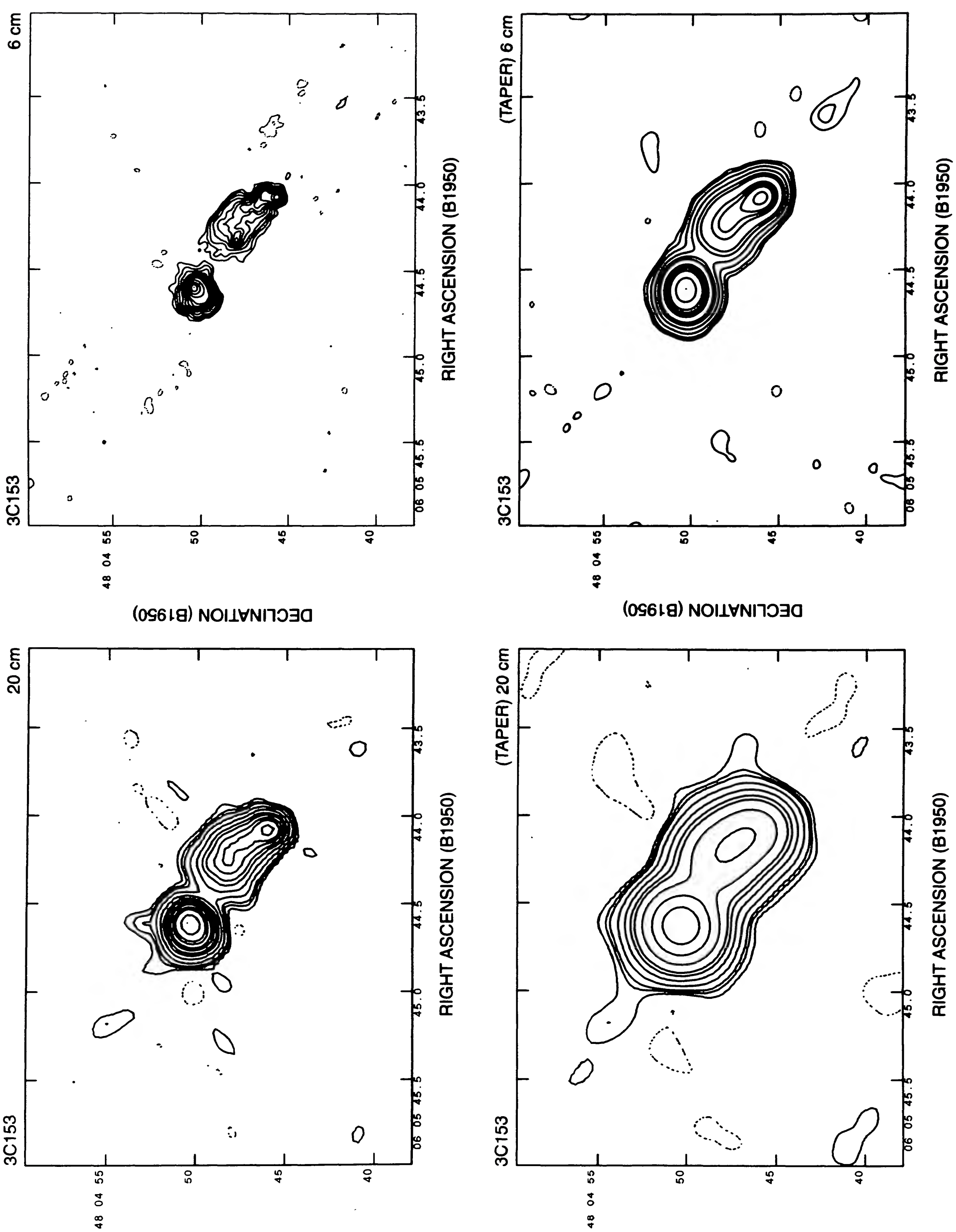

FIG. 1—*Continued*

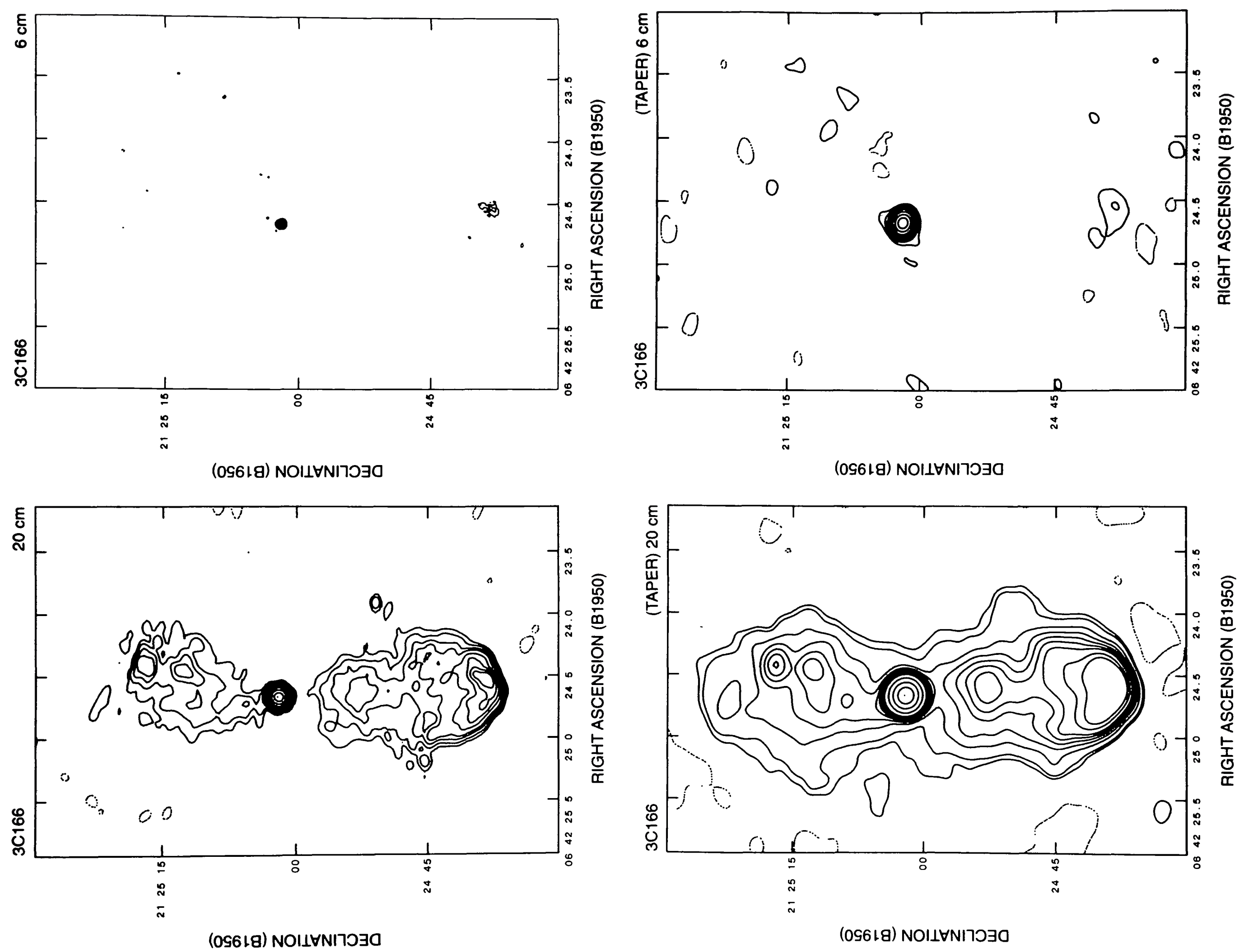

FIG. 1—*Continued*

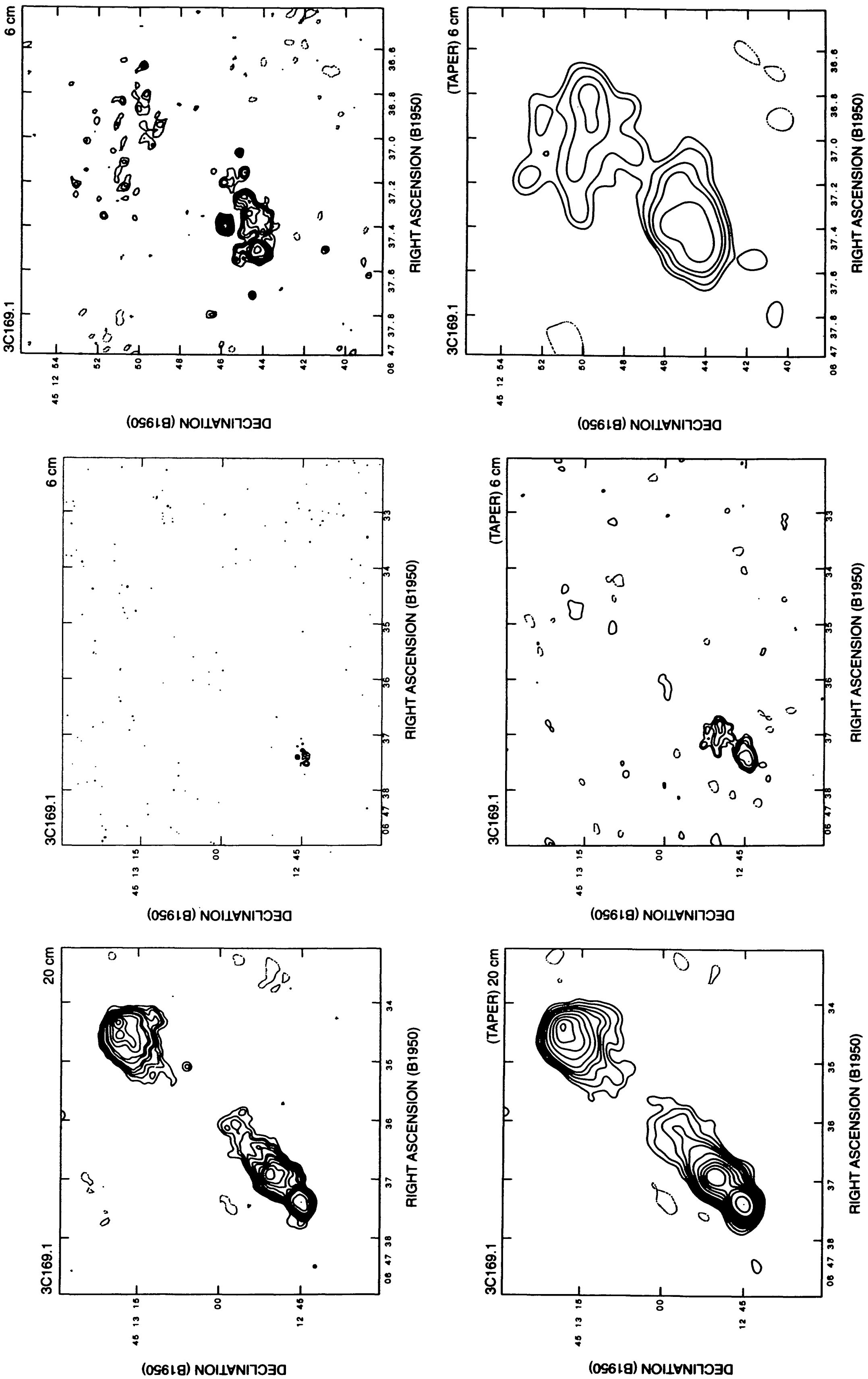

FIG. 1—*Continued*

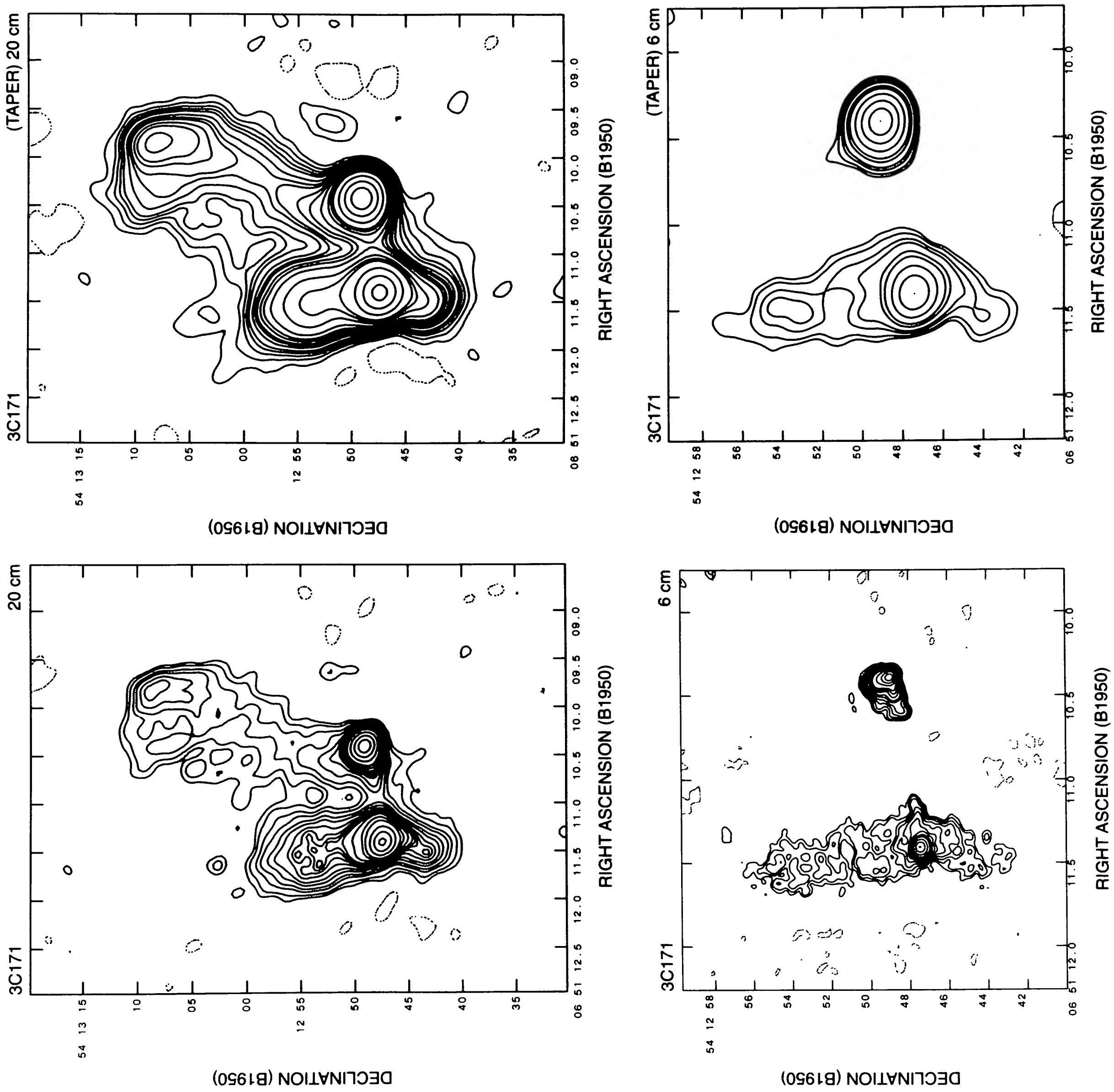

FIG. 1—*Continued*

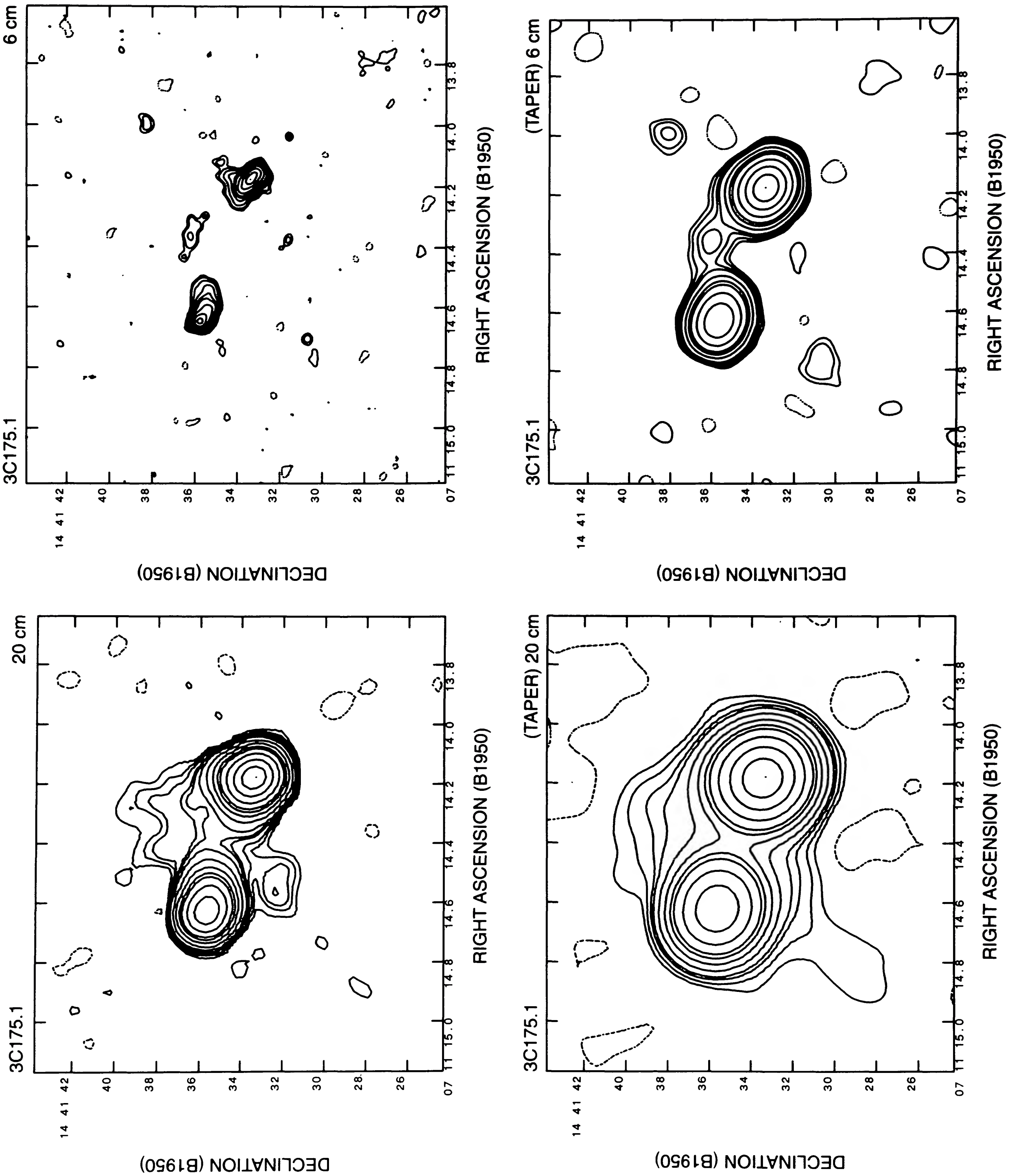

FIG. 1—*Continued*

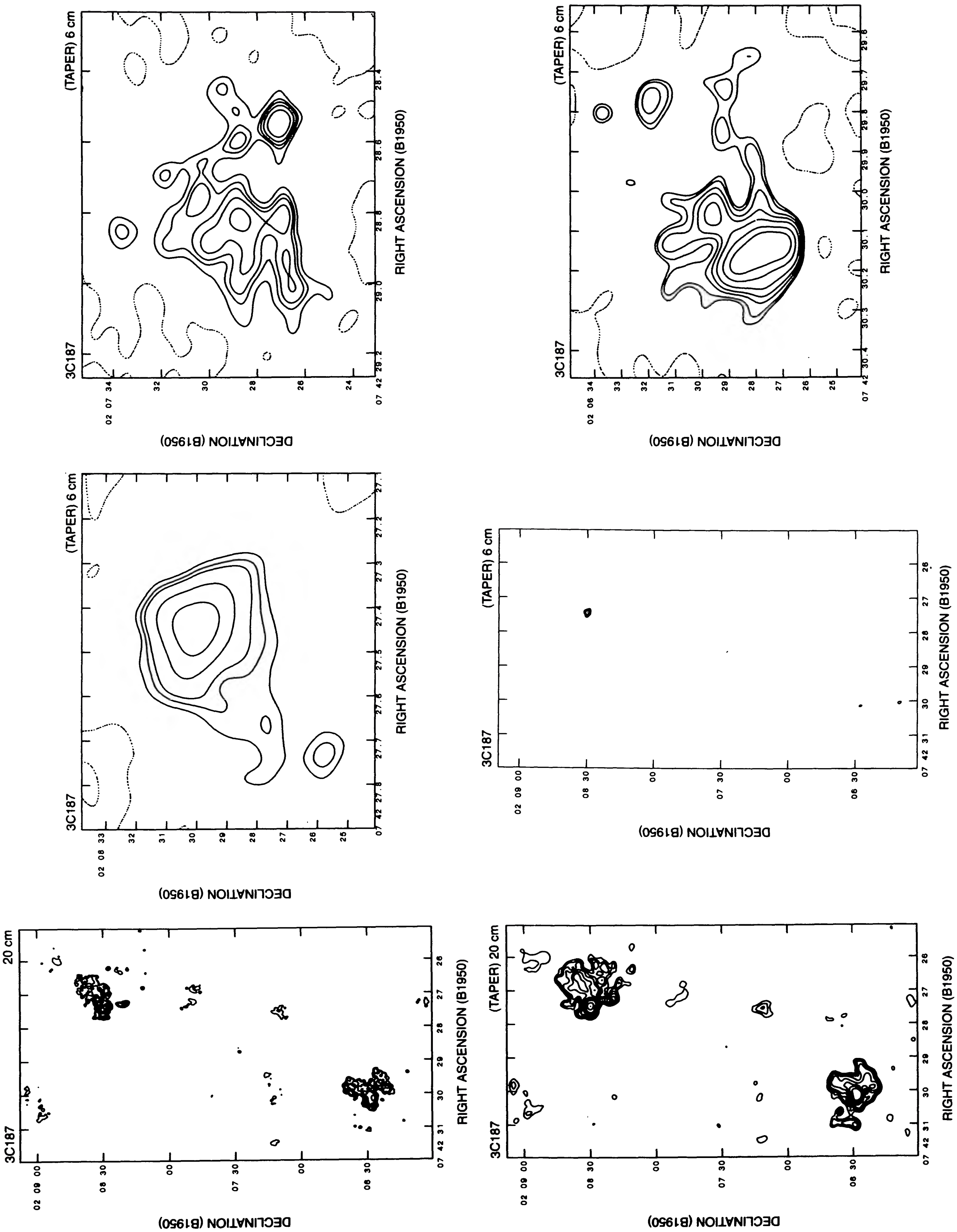

FIG. 1—*Continued*

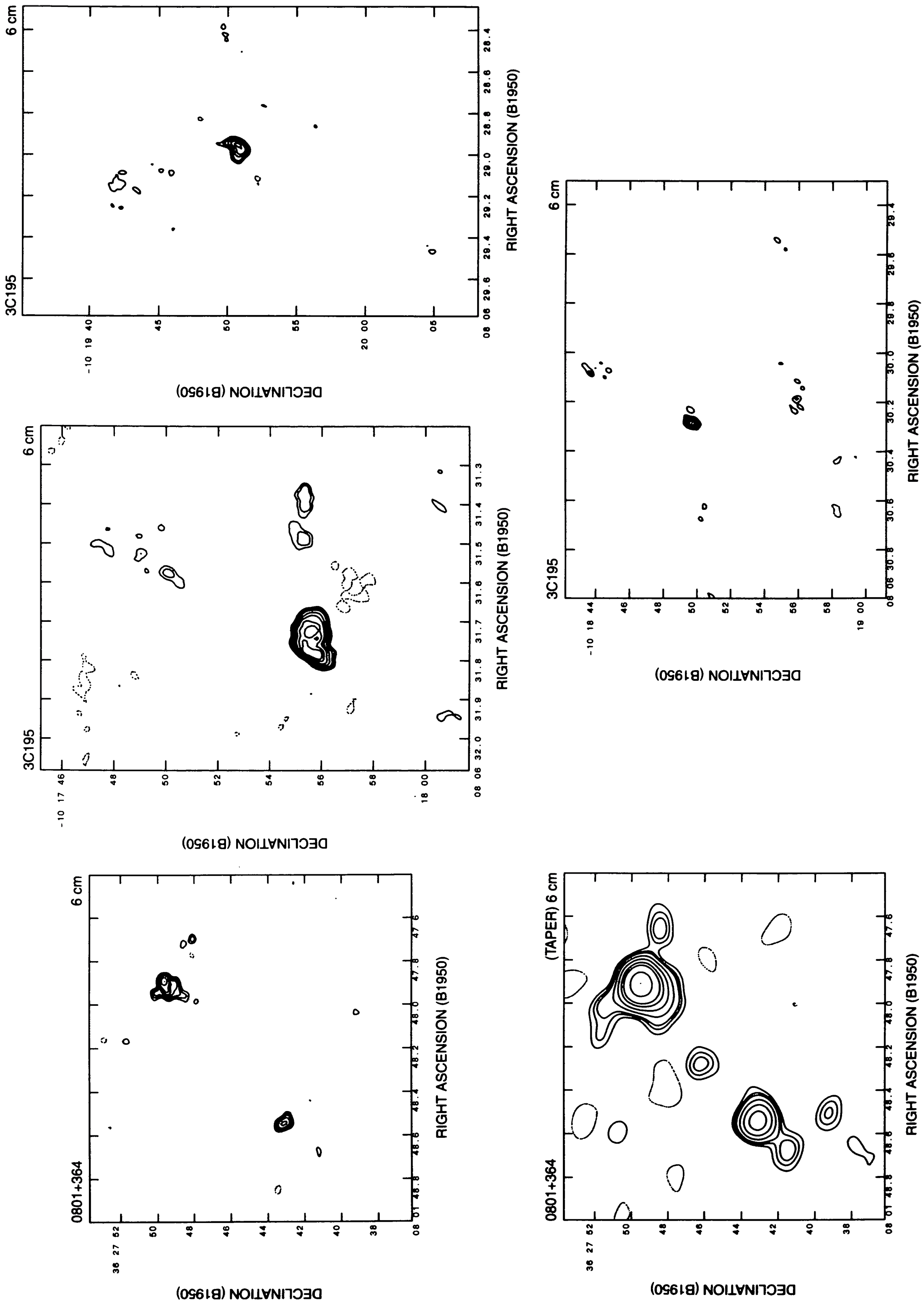

FIG. 1—*Continued*

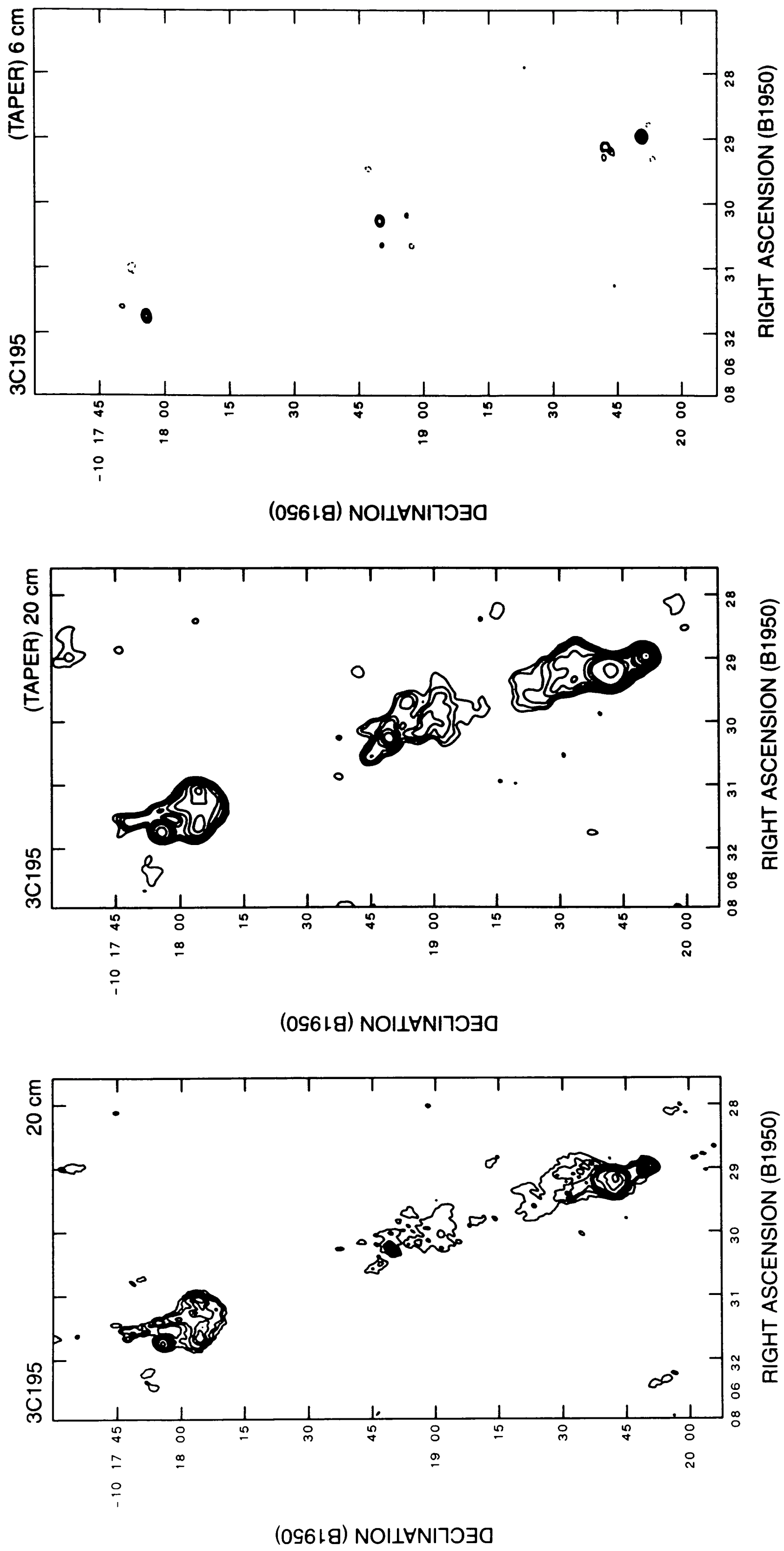

FIG. 1—*Continued*

1995ApJS...99..349N

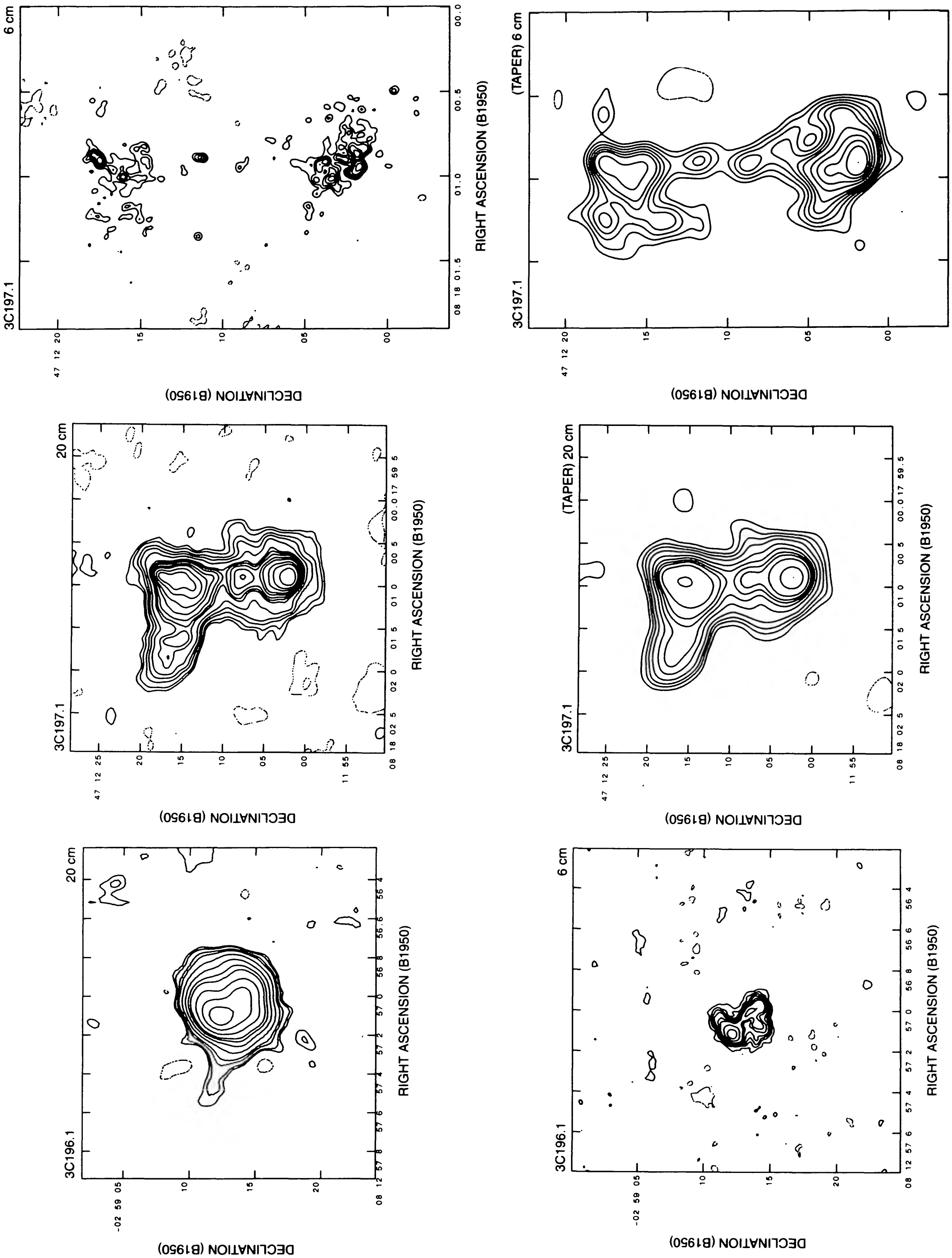

FIG. 1—*Continued*

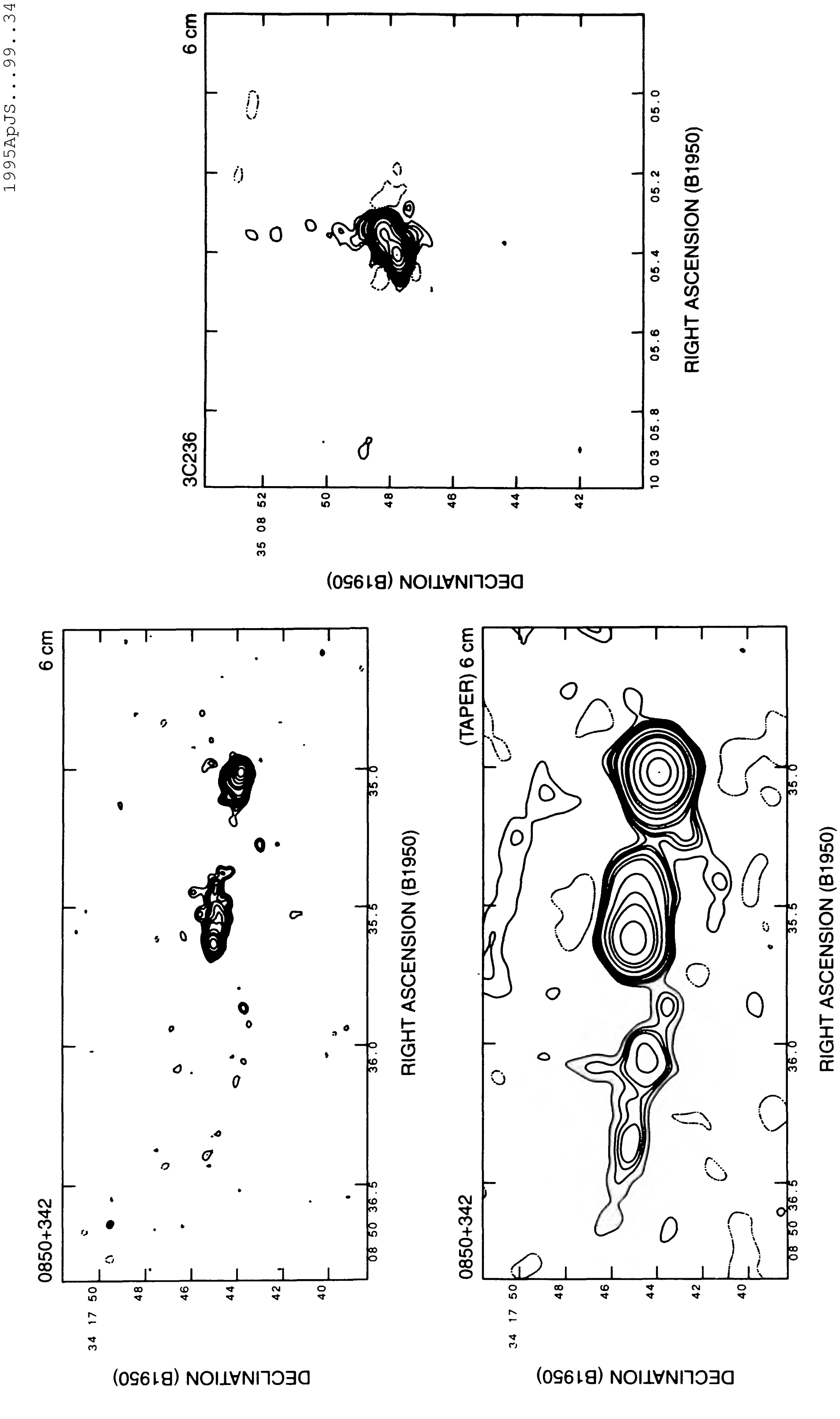

FIG. 1—*Continued*

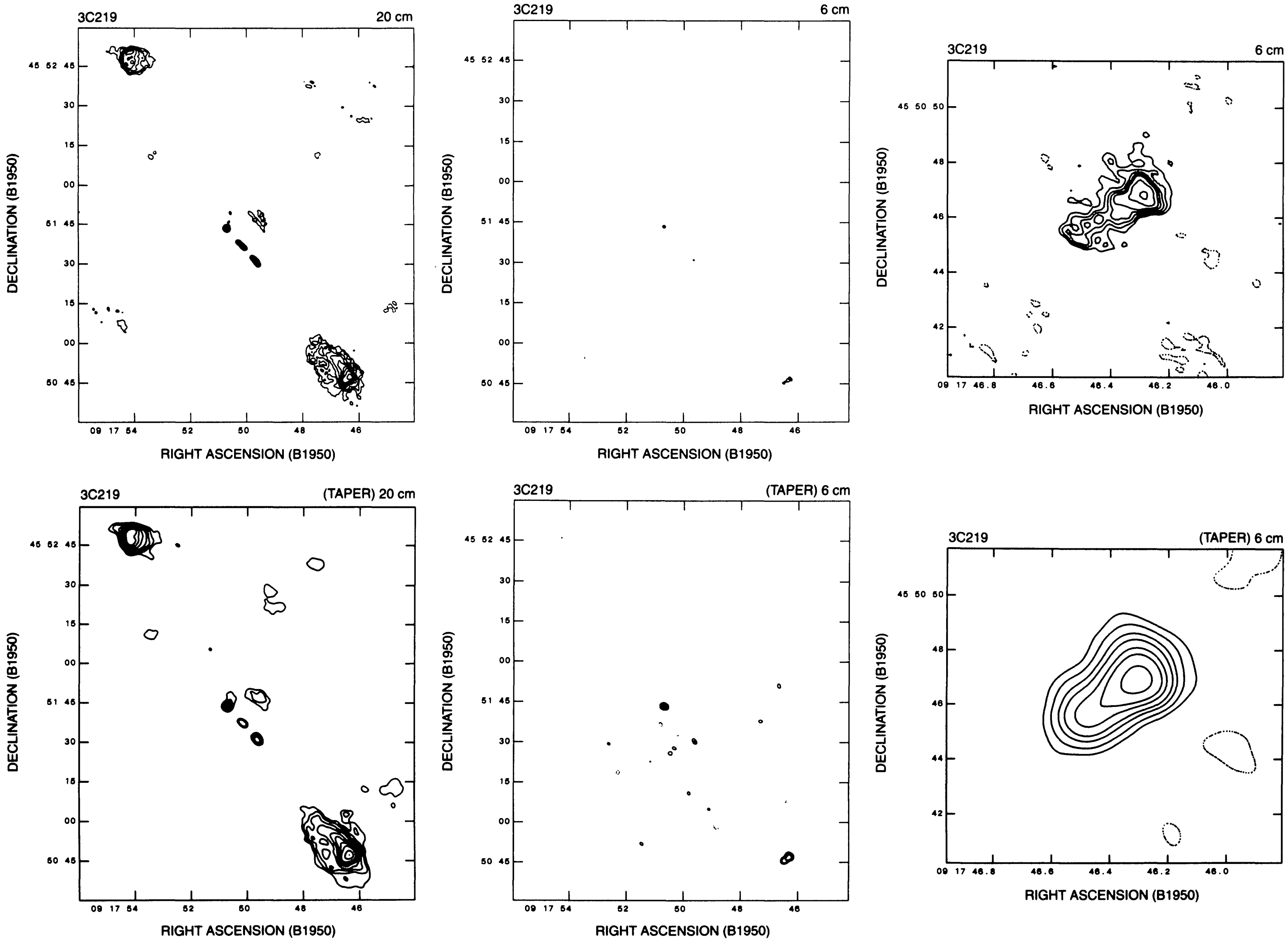

FIG. 1—*Continued*

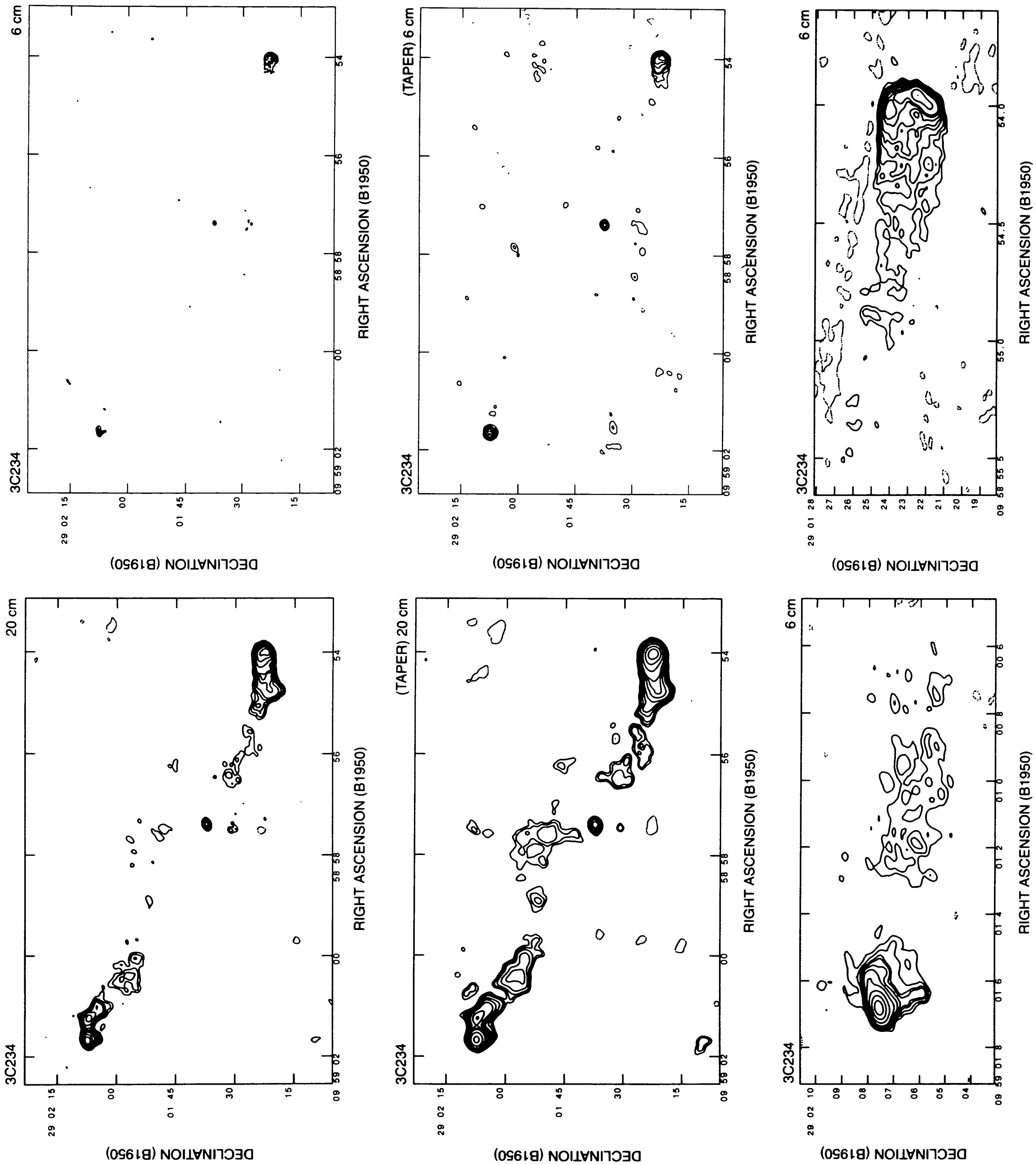

FIG. 1—*Continued*

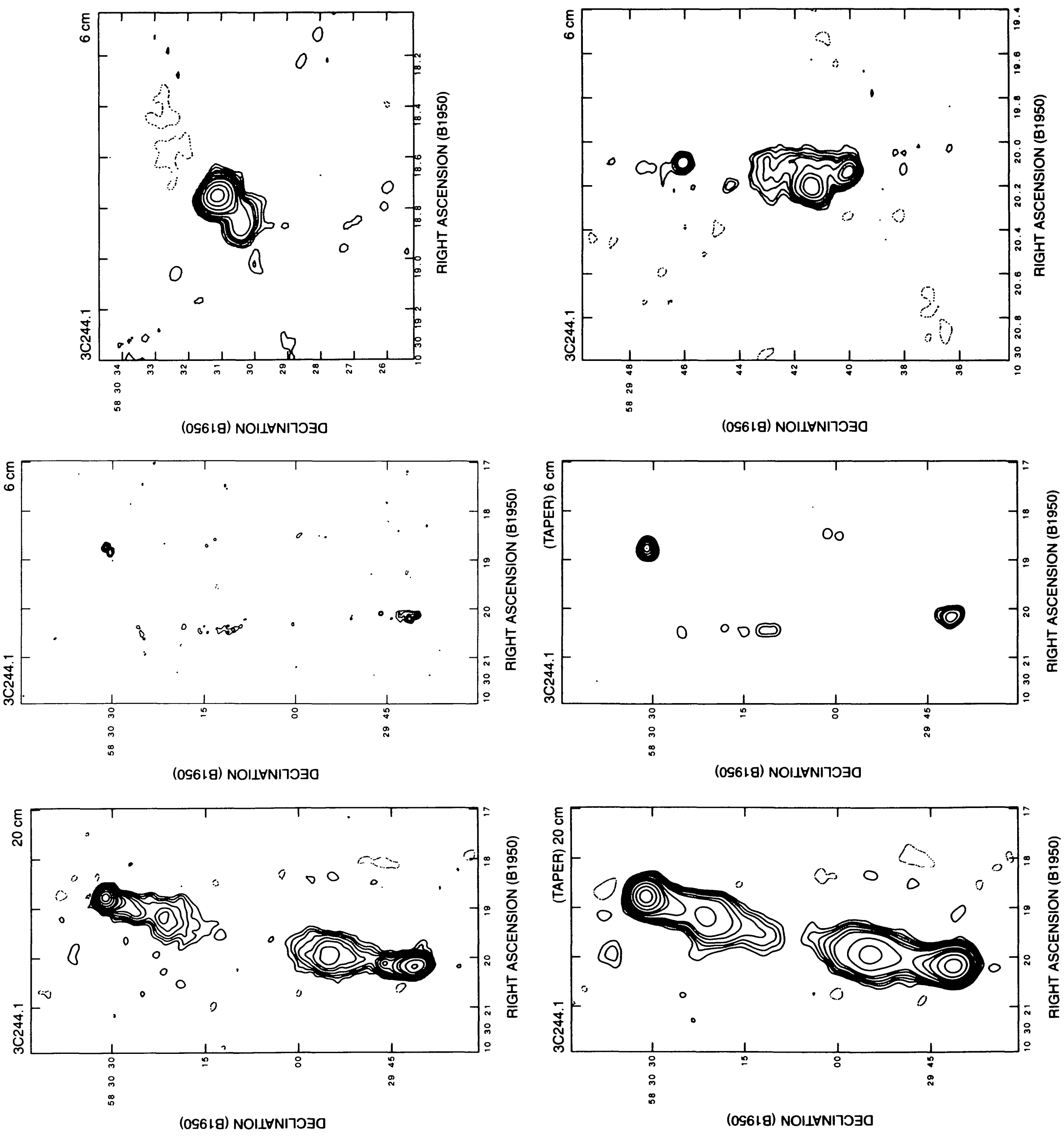

FIG. 1—*Continued*

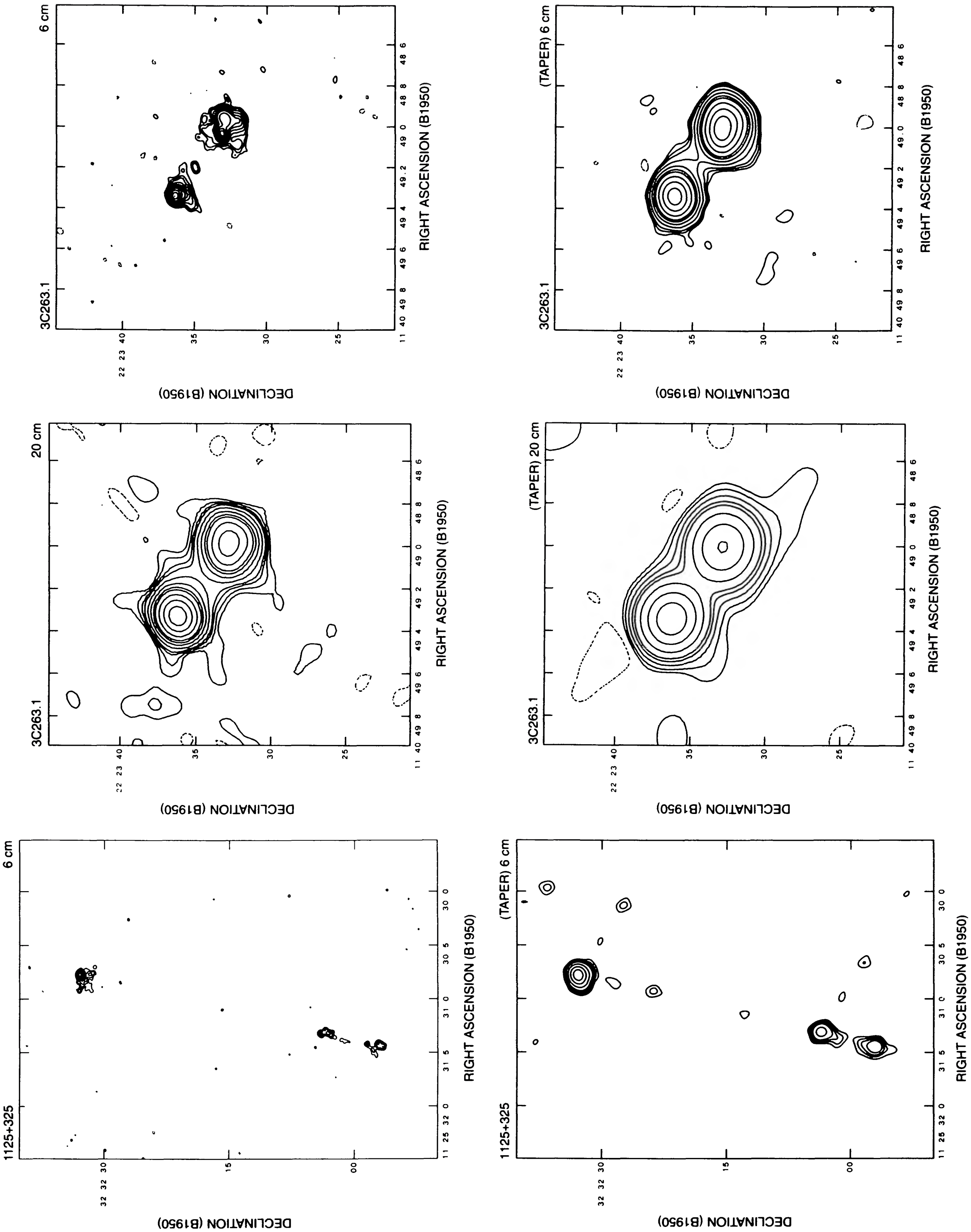

FIG. 1—*Continued*

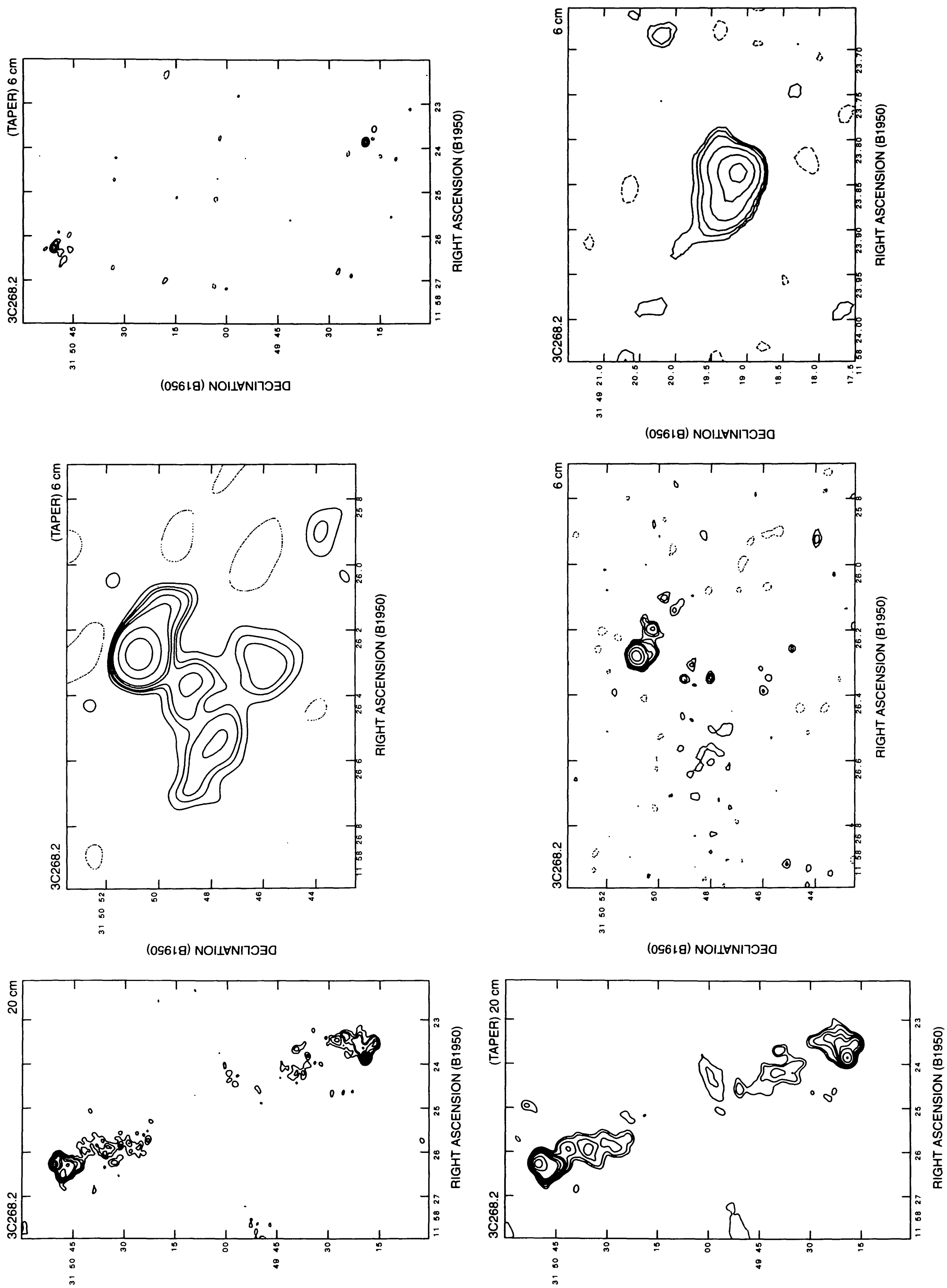

FIG. 1—*Continued*

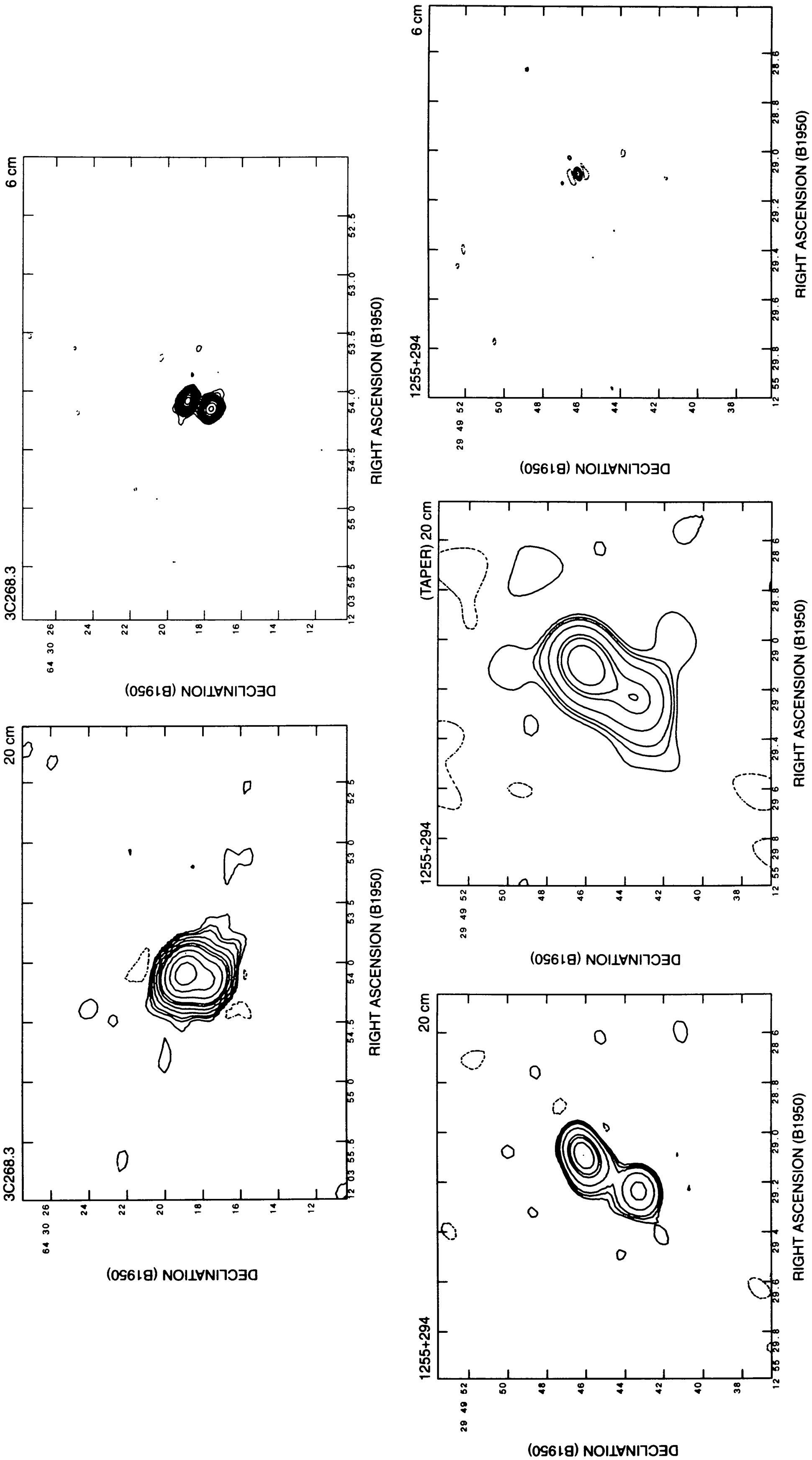

FIG. 1—*Continued*

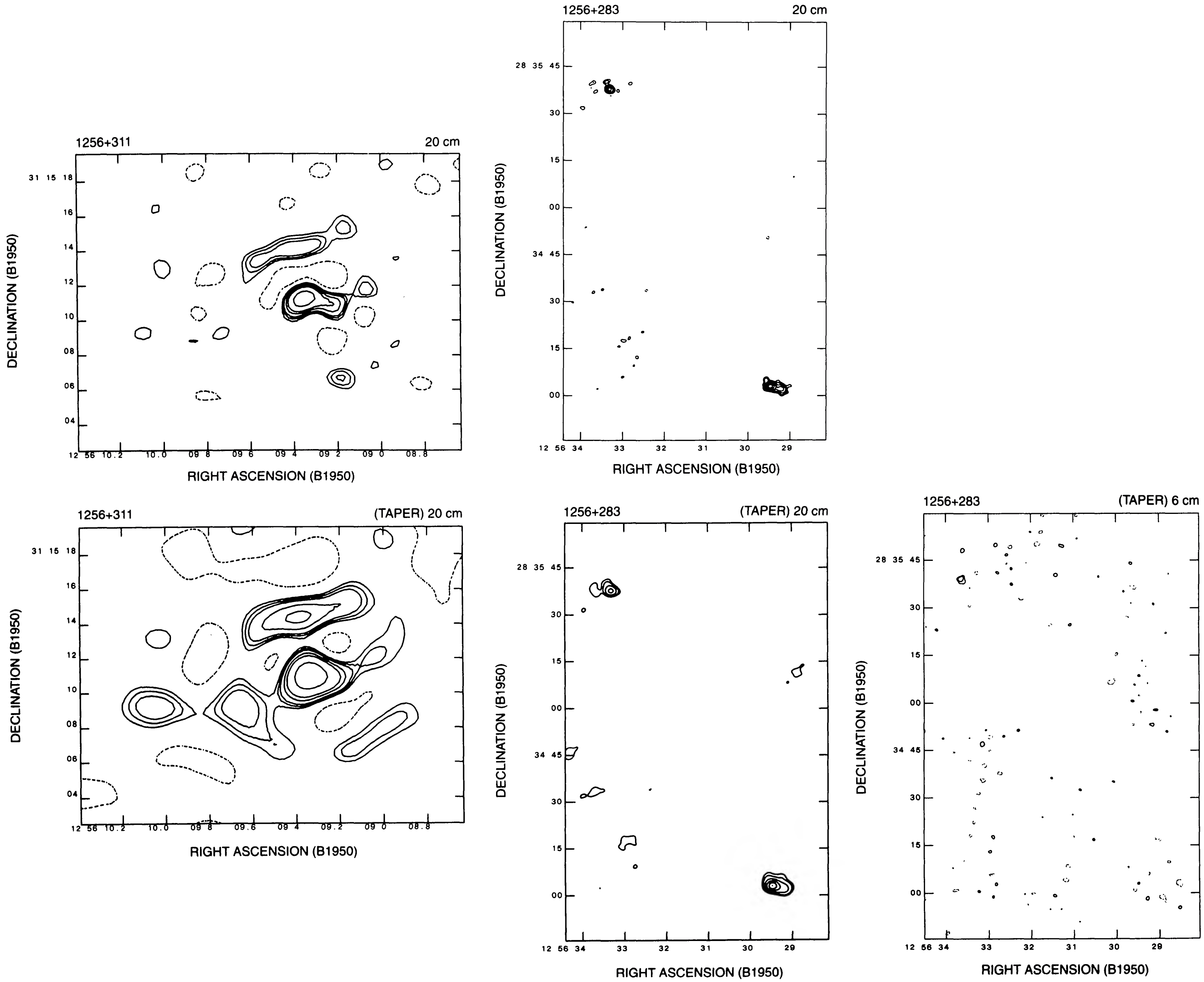

FIG. 1—*Continued*

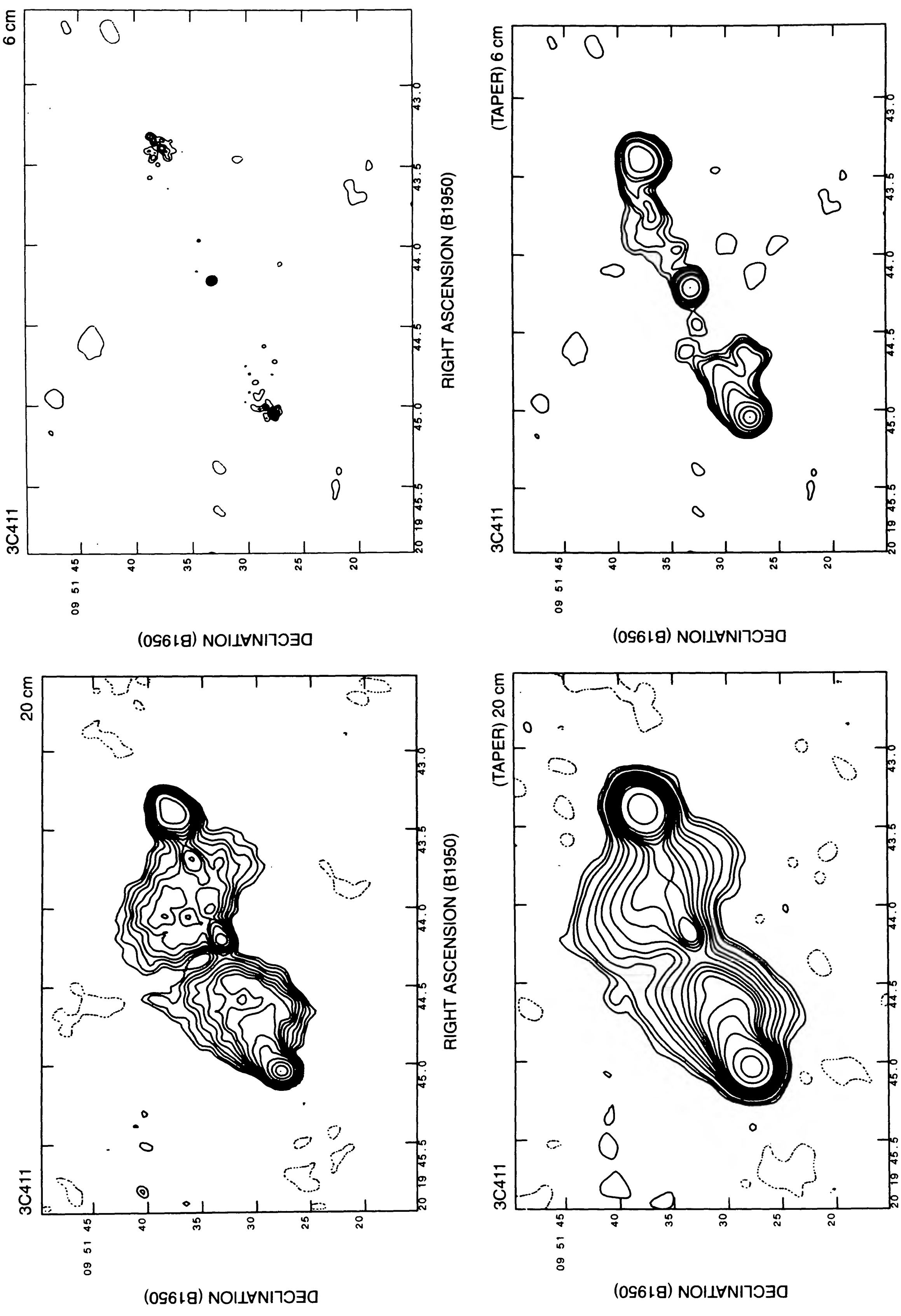

FIG. 1—*Continued*

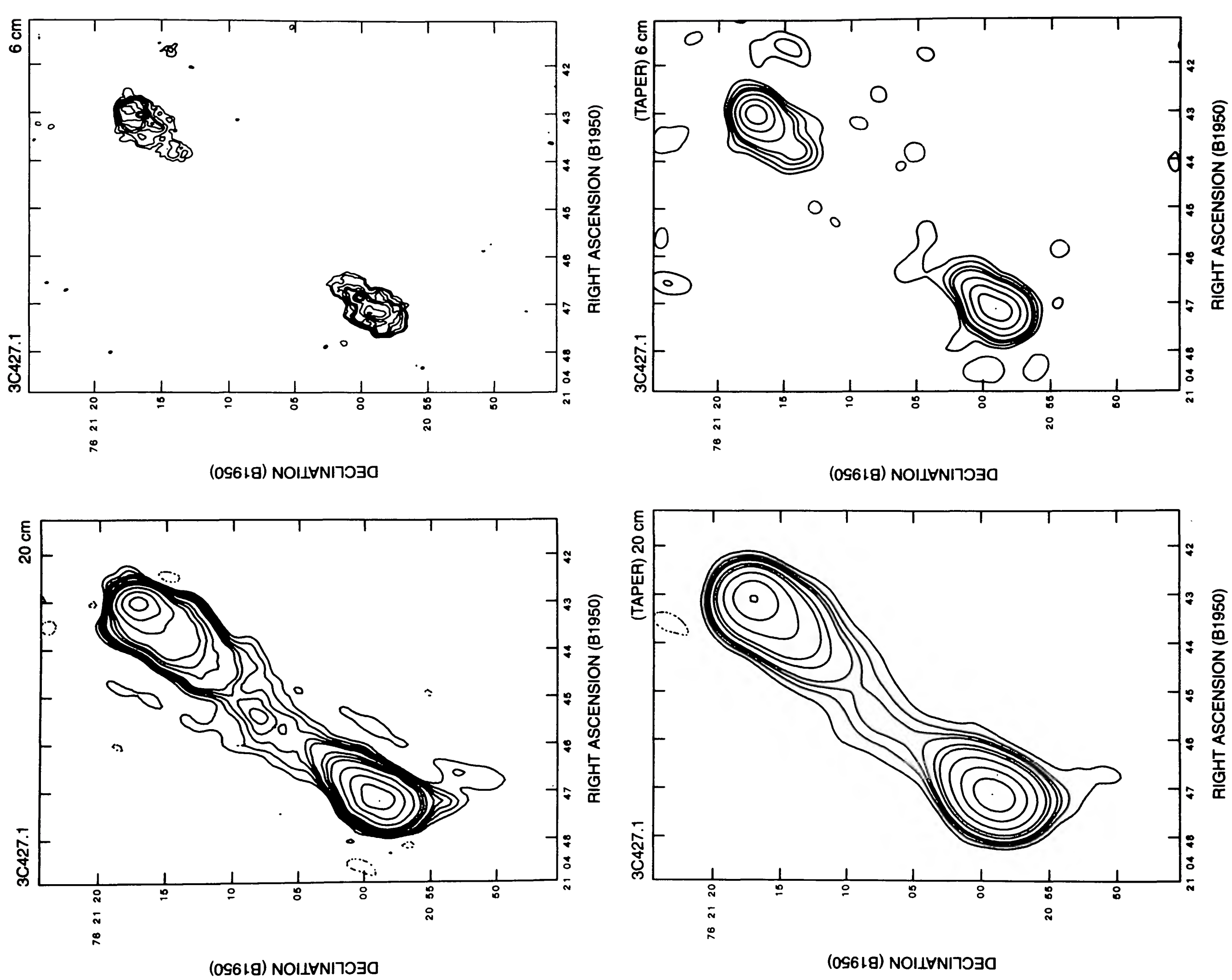

FIG. 1—*Continued*

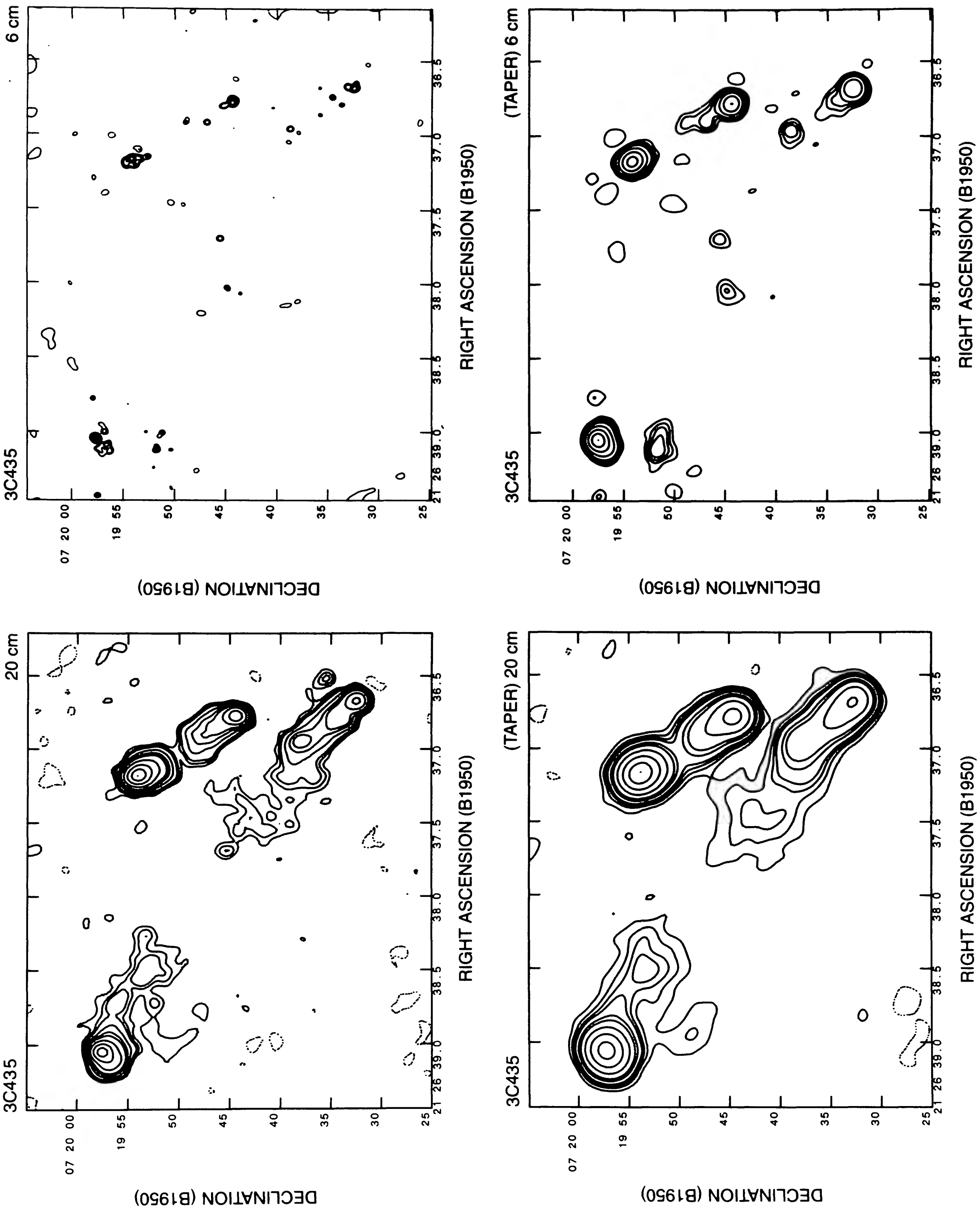

FIG. 1—*Continued*

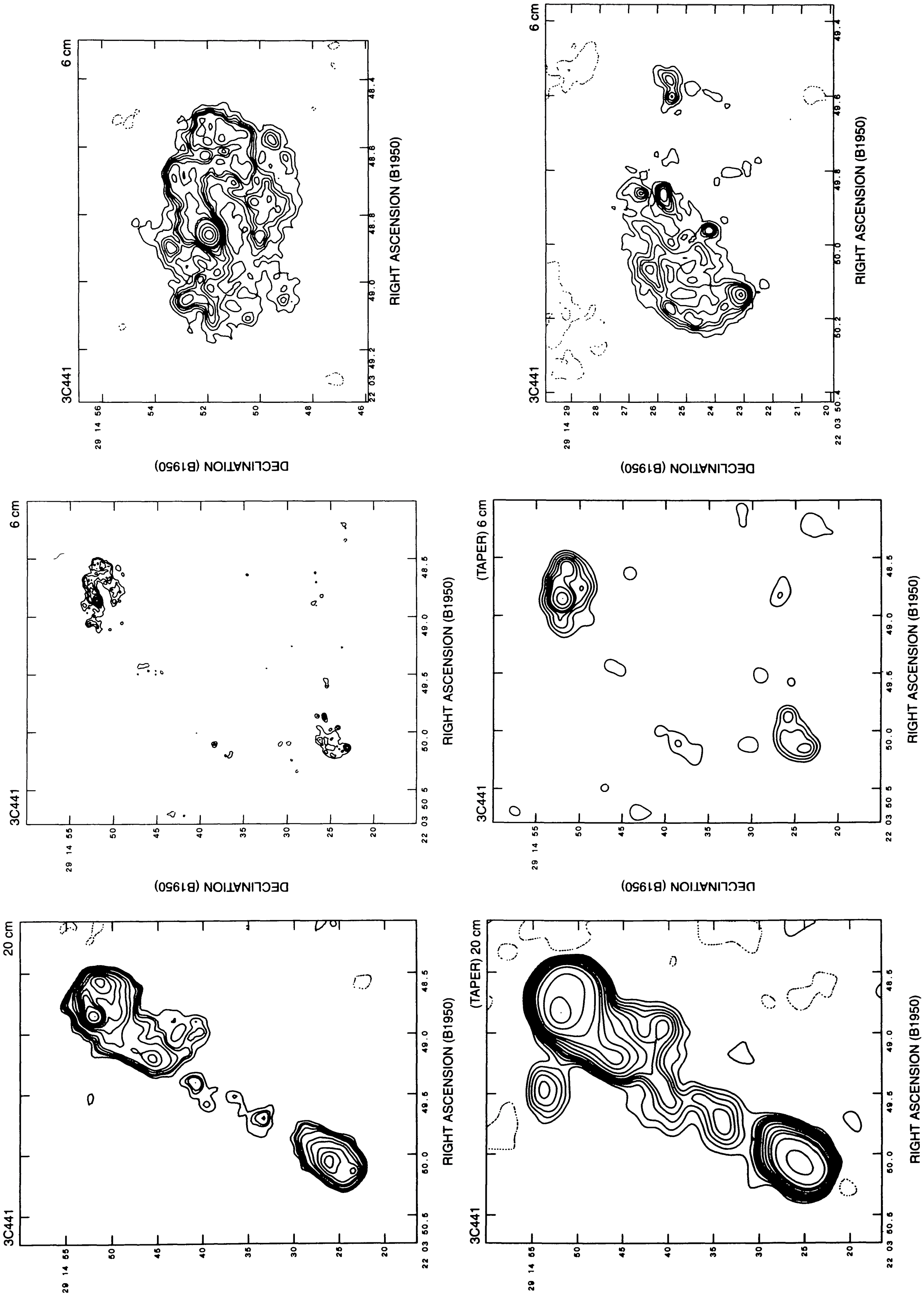

FIG. 1—*Continued*

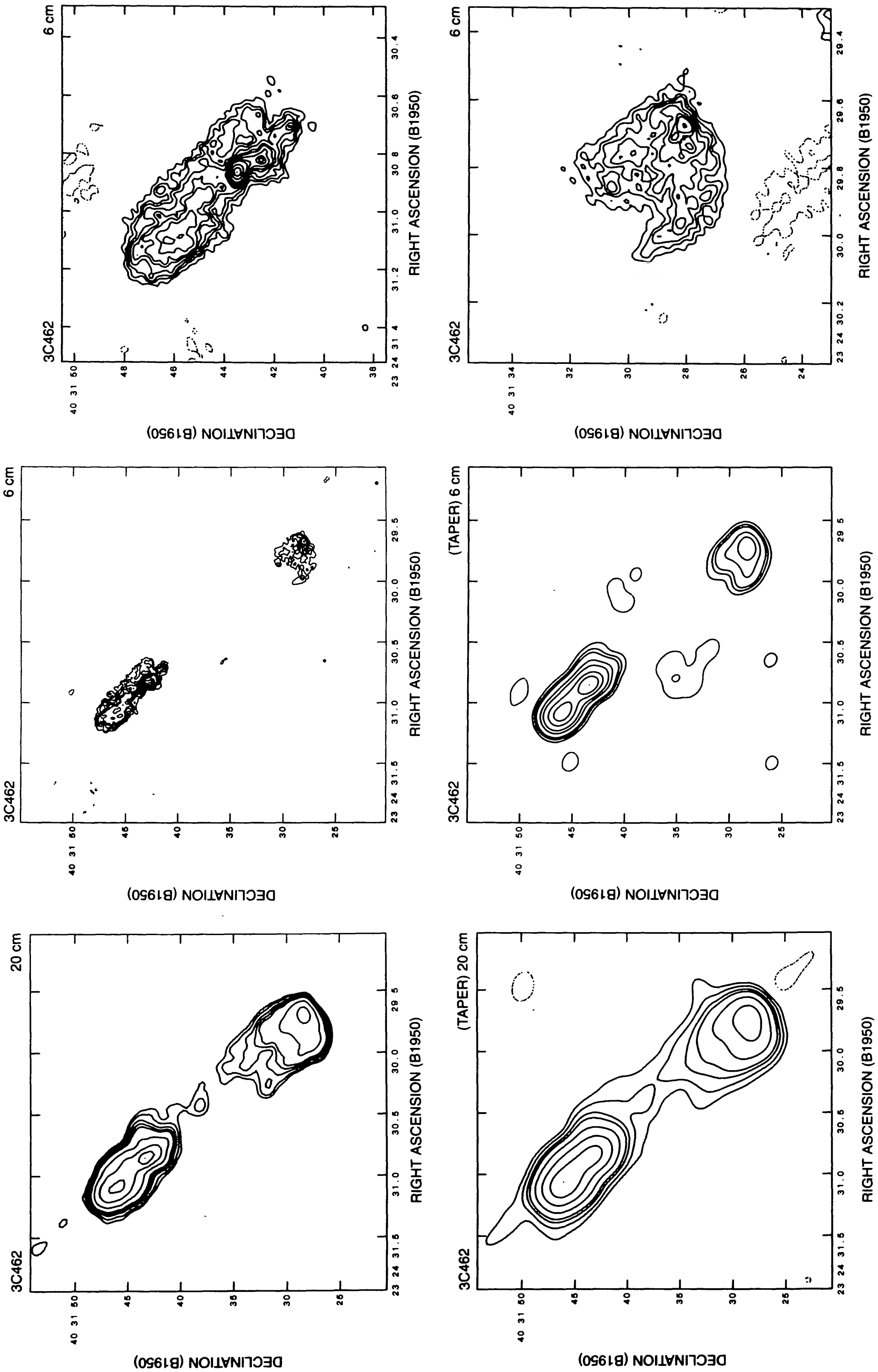

FIG. 1—*Continued*

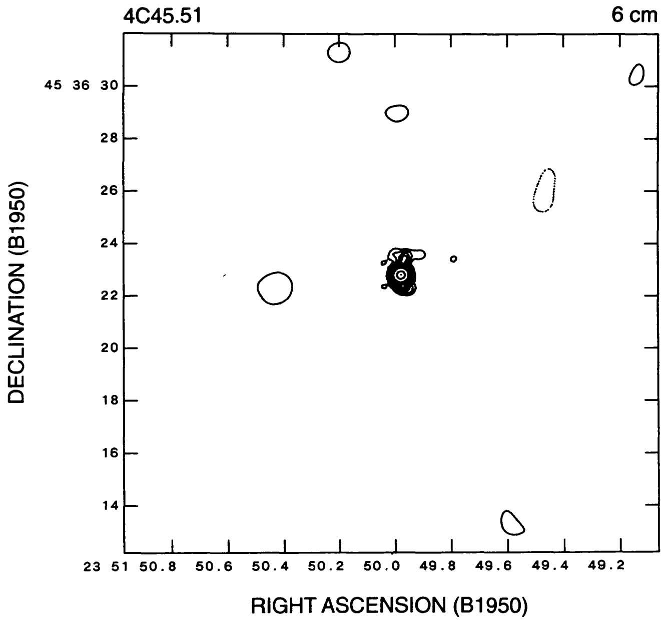

FIG. 1—*Continued*

3C 46.—The northeastern lobe has an unusual string of hot spots, not exactly aligned with the core. There is complex non-aligned structure near the core. Much of the single-dish flux is missing in our data.

3C 49.—This compact source is resolved into two components in the 6 cm map.

3C 61.1.—This has very compact hot spots and faint inner lobe structure. *S*-symmetry suggests changing core orientation.

4C 05.16.—There is complex 6 cm structure in the lobe hot spots.

3C 99.—This is a compact source with triple structure.

3C 105.—Our map shows only the complex structure around the core of this large source.

4C 74.08.—This is a relatively compact source with extreme "splash-back" structure in the main lobes, leading to the formation of extended faint structure orthogonal to the main axis.

3C 123.—No core is visible at the optical galaxy. Two inner bright spots suggest a change in the radio axis. The optical field is crowded, and the northwestern lobe appears to wrap around a galaxy.

3C 132.—This source has strongly edge-brightened lobes with broad faint structure near the (undetected) core. The southeastern lobe appears to wrap around the nearest neighbor galaxy.

3C 153.—The source has curved radio structure approximately orthogonal to the host galaxy long axis.

3C 166.—This is a strong core source with broad lobes. The northern lobe appears to run into a faint galaxy. A brighter galaxy lies to the side of the southern lobe hot spot.

3C 169.1.—The 6 cm map shows multiple hot spots in the lobes of this large source.

3C 171.—Faint lobe structure appears to splash off walls on either side of this unusual source. Our CCD image shows optical structure bending at the eastern wall too, and an optical bright spot along the western radio jet, inside the hot spot. Heckman, van Breugel, & Miley (1984) find line emission at these locations. The walls are not visible in optical light.

OI 417.—This compact source lies within the optical host galaxy. The slight radio extension does not correspond to the direction of any of four close companion galaxies.

3C 175.1.—This is a compact double source with some faint structure orthogonal to the main (curved) axis.

3C 187.—This is a large double-lobe source with complex structure in both. The galaxy lies in a rich cluster with over 30 members projected between the radio lobes.

0755+480, 0801+364.—These are faint sources at mid-range redshift, with no outstanding structures.

3C 195.—This is a large double-lobe source with bright hot spots and complex lobe structure, suggesting small radio-axis changes. The core is bright and has extended structures on both sides. The galaxy has an optical extension or jet orthogonal to the radio, but the inner isophotes are along the radio axis. Much of the inner radio structure lies within the host galaxy.

3C 196.1.—This is a compact and complex one-sided source that lies well within the host galaxy. The galaxy is considerably elongated along the radio axis and has a second "nucleus" on the side opposite the radio extension.

3C 197.1.—The radio structure is comparable in size with the host galaxy and oriented orthogonal to the optical axis. There is a string of compact knots and the nucleus approximately in a line, and the outer radio structure to the north suggests deflection by a large wall.

3C 55.16.—This compact source is extended approximately orthogonal to the long axis of the large host galaxy.

3C 219.—This large source has narrow jetlike sections to the southwest, from a bright core.

3C 223.—Our observations show only the weak core of this very large double-lobe source.

3C 234.—This large source has narrow lobes and *S*-symmetry just inside the hot spots.

3C 236.—We detect only the core structure of this giant radio source. VLBI structure aligns with the VLA map and overall structure.

3C 244.1.—There is slight *C*-symmetry in the elongated lobes of this source.

3C 258.—We detect only an unresolved core from this large source.

1125+325.—We have only a 6 cm map, showing a weak core and compact hot spots in a large double-lobe source.

3C 263.1.—The source has is a weak core and compact lobes.

3C 268.2.—This source has no detected core and unresolved bright hot spots in the lobes. There is narrow faint structure inside the lobes.

3C 268.3.—This is a compact one-sided source resolved at 6 cm.

1253+292, 1256+298, 1256+312.—These are weak compact sources. We are not sure of detection in the last one. We do not have redshifts for any of these.

1256+283.—This is a wide double with no detected core.

3C 411.—The source has bright compact hot spots and core and faint splash-back structure.

TABLE 2

PROPERTIES OF RADIO GALAXY MAPS

Source, Map	Restoring Beam (arcsec)	Position Angle	Noise (mJy)	Peak Flux (mJy)	Levels (percent of peak flux)
3C6.1 C	0.5 x 0.3	-17	0.5	175.1	-0.1,0.1,0.3,0.7,1,1.5,2,5,10,20,40,60,90
3C6.1 C tap	1.6 x 1.5	10	0.9	395.3	-0.07,0.07,0.1,0.15,0.3,0.5,0.7,1,2,4,7,10,20,40,60,90
3C6.1 L	1.6 x 1.0	-15	0.8	1124.9	-0.02,0.02,0.04,0.07,0.1,0.15,0.2,0.3,0.4,0.7,1,2,5,10,20,40,60,90
3C6.1 L tap	2.7 x 2.2	-15	1.2	1281.4	-0.02,0.02,0.04,0.07,0.1,0.2,0.4,0.7,1,2,4,7,10,20,40,60,90
54W067 C	0.4 x 0.4	-5	0.3	6.5	
54W067 C tap	1.6 x 1.6	51	0.5	3.1	
54W067 L	1.3 x 1.2	5	0.4	174.1	-0.6,0.6,0.8,1,1.5,2,3,4,7,10,20,40,60,90
54W067 L tap	2.4 x 2.4	40	0.7	229.4	-0.8,0.8,1.1,1.5,2,3,4,5,6,8,10,20,40,60,90
54W068 C	0.4 x 0.4	37	0.3	6.6	
54W068 C tap	1.6 x 1.4	69	0.6	3.3	
54W068 L	1.3 x 1.2	7	1.2	46.2	-1,1,2,4,7,10,20,40,60,90
54W068 L tap	2.5 x 2.4	35	2.8	102.5	-1,1,2,4,7,10,20,40,60,90
54W084 L	1.4 x 1.2	2	0.2	3.2	-3,3,5,7,10,20,40,60,90
54W084 L tap	2.5 x 2.5	35	0.3	1.8	-6,6,8,10,20,40,60,90
OB343 C	0.4 x 0.4	47	0.7	1222.0	
OB343 C tap	1.7 x 1.5	63	0.9	1223.9	
OB343 L	1.2 x 1.2	41	0.5	1856.0	
OB343 L tap	2.5 x 2.4	55	3.2	1856.5	
0027-286 L	2.7 x 1.1	-2	0.3	4.6	
0027-286 L tap	3.5 x 2.2	-1	0.3	4.1	
3C34 C	0.4 x 0.4	56	0.2	8.8	-0.7,0.7,1.1,2,4,7,10,20,40,60,90
3C34 C upper lobe					-0.4,0.4,0.5,0.6,0.8,1,1.2,1.6,2,2.5,3,4,7,10,20,40,60,90
3C34 C lower lobe					-0.3,0.3,0.4,0.5,0.6,0.8,1,2,4,7,10,20,40,60,90
3C34 C tap	1.7 x 1.4	67	0.3	4.0	-0.7,0.7,1.1,1.4,1.7,2,3,4,7,10,20,40,60,90
3C34 L	1.4 x 1.4	47	1.1	106.5	-0.2,0.2,0.35,0.55,0.75,1,1.2,1.5,2,4,7,10,20,40,60,90
3C34 L tap	2.5 x 2.5	59	2.3	190.4	-0.2,0.2,0.35,0.55,0.75,1,1.2,1.5,2,4,7,10,20,40,60,90
3C41 C	0.4 x 0.4	34	0.6	121.8	-0.2,0.2,0.3,0.4,0.7,1,1.5,2,4,7,10,20,40,60,90
3C41 C tap	1.6 x 1.5	67	0.8	435.1	-0.1,0.1,0.2,0.4,0.7,1,2,4,7,10,20,40,60,90
3C41 L	1.3 x 1.1	15	1.2	705.9	-0.05,0.05,0.07,0.1,0.15,0.2,0.3,0.4,0.7,1,2,4,7,10,20,40,60,90
3C41 L tap	2.4 x 2.4	40	2.5	1097.2	-0.04,0.04,0.07,0.1,0.2,0.4,0.7,1,2,4,7,10,20,40,60,90
3C46.0 C	0.4 x 0.4	47	0.2	4.1	
3C46.0 C tap	1.5 x 1.4	52	0.4	14.2	-1,1,2,4,7,10,20,40,60,90
3C46.0 L	1.1 x 1.1	35	0.3	34.2	-0.4,0.4,0.7,1,2,4,7,10,20,40,60,90
3C46.0 L tap	2.3 x 2.3	43	0.8	64.0	-0.4,0.4,0.5,0.7,1,2,4,7,10,20,40,60,90
3C49 C	0.4 x 0.4	18	1.3	600.7	-0.05,0.05,0.07,0.1,0.2,0.4,0.7,1,2,4,7,10,20,40,60,90
3C49 C tap	1.6 x 1.5	61	0.9	780.0	
3C49 L	1.4 x 1.3	-10	2.5	2083.2	
3C49 L tap	2.6 x 2.6	26	1.7	2428.5	
3C61.1 C	0.6 x 0.3	14	0.4	28.1	
3C61.1 C upper lobe					-0.5,0.5,0.7,1,2,4,7,10,20,40,60,90
3C61.1 C lower lobe					-0.5,0.5,0.7,1,2,3,4,7,10,20,40,60,90
3C61.1 C tap	1.3 x 1.2	28	0.7	108.4	-0.4,0.4,0.7,1,2,4,7,10,20,40,60,90
3C61.1 L	1.9 x 1.0	13	1.0	360.0	
3C61.1 L upper lobe					-0.08,0.08,0.12,0.15,0.2,0.4,0.7,1,1.3,2,4,7,10,20,40,60,90
3C61.1 L lower lobe					-0.07,0.07,0.1,0.2,0.4,0.7,1,2,4,7,10,20,40,60,90
3C61.1 L tap	2.9 x 2.2	14	2.4	758.3	-0.15,0.15,0.2,0.4,0.7,1,2,4,7,10,20,40,60,90
4C05.16 C	0.4 x 0.4	23	0.6	312.8	-0.07,0.07,0.2,0.6,1,2,4,7,10,20,40,60,90
4C05.16 C upper lobe					-0.035,0.035,0.045,0.06,0.08,0.1,0.15,0.2,0.3,0.5,0.7,0.8,1,2,4,7,10,20,40
4C05.16 C lower lobe					-0.04,0.04,0.07,0.1,0.12,0.16,0.2,0.25,0.3,0.5,0.7,1,2,4,7,10,20,40,60,90
4C05.16 C tap	1.7 x 1.5	73	0.6	542.1	-0.07,0.07,0.1,0.2,0.4,0.7,1,2,4,7,10,20,40,60,90
4C05.16 L	1.5 x 1.3	-8	2.2	1291.6	-0.07,0.07,0.1,0.2,0.4,0.7,1,2,4,7,10,20,40,60,90
4C05.16 L tap	2.6 x 2.5	17	3.4	1507.3	-0.1,0.1,0.2,0.4,0.7,1,2,4,7,10,20,40,60,90
3C99 C	0.5 x 0.4	9	0.2	258.1	-0.03,0.03,0.05,0.07,0.1,0.2,0.4,0.7,1,2,4,7,10,20,40,60,90
3C99 C tap	1.6 x 1.6	51	0.5	412.5	-0.04,0.04,0.05,0.07,0.1,0.2,0.4,0.7,1,2,4,7,10,20,40,60,90
3C99 L	1.5 x 1.2	-7	0.9	1128.8	-0.03,0.03,0.07,0.1,0.15,0.2,0.3,0.4,0.7,1,2,4,7,10,20,40,60,90
3C99 L tap	2.6 x 2.5	3	1.3	1361.8	-0.04,0.04,0.07,0.1,0.2,0.4,0.7,1,2,4,7,10,20,40,60,90
3C105 C	0.5 x 0.4	2	0.6	144.0	-0.15,0.15,0.2,0.3,0.4,0.6,0.8,1,2,4,7,10,20,40,60,90
3C105 C (enlargement)					-0.15,0.15,0.2,0.3,0.4,0.6,0.8,1,2,4,7,10,20,40,60,90
3C105 C tap	1.7 x 1.6	64	1.9	429.9	-0.15,0.15,0.3,0.5,0.7,1,2,4,7,10,20,40,60,90
3C105 L	1.5 x 1.3	-7	1.0	830.9	-0.04,0.04,0.055,0.07,0.09,0.12,0.14,0.17,0.2,0.25,0.3,0.4,0.7,1,2,4,7,10
3C105 L tap	2.6 x 2.5	23	1.4	138.3	-0.04,0.04,0.055,0.07,0.09,0.12,0.14,0.17,0.2,0.25,0.3,0.4,0.7,1,2,4,7,10
4C74.08 C	0.6 x 0.5	49	0.6	76.9	-0.2,0.2,0.25,0.35,0.47,0.55,0.67,0.85,0.95,1.2,1.6,2,3,4,7,10,20,40,60,90
4C74.08 C tap	1.7 x 1.4	70	2.1	137.6	-0.3,0.3,0.4,0.7,1.2,2,3,5,7,10,20,40,60,90
4C74.08 L	1.1 x 1.1	42	0.8	303.3	-0.07,0.07,0.1,0.15,0.2,0.3,0.5,0.7,1,1.5,2,2.5,3,3.5,5,7,10,20,40,60,90
4C74.08 L tap	2.3 x 2.2	40	1.6	518.1	-0.07,0.07,0.12,0.2,0.25,0.3,0.4,0.7,1,2,4,5,7,10,20,40,60,90
3C123 C	0.4 x 0.4	51	15.1	1411.5	-0.3,0.3,0.75,1.5,2.5,4,7,10,20,40,60,90
3C123 C tap	1.6 x 1.5	56	60.8	4390.5	-0.4,0.4,0.7,1,2,4,7,10,20,40,60,90
3C123 L	1.3 x 1.2	39	44.7	8646.3	-0.15,0.15,0.2,0.25,0.32,0.4,0.5,0.55,0.6,0.7,1,2,4,7,10,20,40,60,90
3C123 L tap	2.6 x 2.5	63	128.6	116.7	-0.4,0.4,0.5,0.65,0.85,1,1.2,1.4,2,4,7,10,20,40,60,90

1995ApJS...99..349N

TABLE 2—*Continued*

Source, Map	Restoring Beam (arcsec)	Position Angle	Noise (mJy)	Peak Flux (mJy)	Levels (percent of peak flux)
3C132 C	0.4 x 0.4	86	0.7	67.0	-0.25,0.25,0.3,0.4,0.5,0.6,0.8,1,1.5,2,4,7,10,20,40,60,90
3C132 C tap	1.7 x 1.5	68	2.2	129.2	-0.2,0.2,0.4,0.6,0.8,1,1.5,2,4,7,10,20,40,60,90
3C132 L	1.4 x 1.3	-14	0.9	310.4	-0.06,0.06,0.08,0.1,0.15,0.2,0.4,0.6,0.8,1,1.5,1.7,2,2.5,3,4,7,10,20,40,60,90
3C132 L tap	2.6 x 2.5	-90	2.0	599.3	-0.04,0.04,0.055,0.08,0.14,0.24,0.4,0.7,1,1.5,2,3,4,7,10,20,40,60,90
OG3 C	0.5 x 0.4	-12	1.4	1776.5	
OG3 C tap	1.6 x 1.5	82	3.4	1889.1	
OG3 L	1.5 x 1.3	-11	0.7	2214.3	
OG3 L tap	2.6 x 2.6	48	3.1	2226.8	
3C153 C	0.5 x 0.4	54	0.6	239.8	-0.06,0.06,0.1,0.17,0.27,0.4,0.53,0.65,0.8,1,2,4,7,10,20,40,60,90
3C153 C tap	1.7 x 1.4	77	1.4	485.9	-0.06,0.06,0.1,0.2,0.4,0.7,1,2,2.5,3,4,7,10,20,40,60,90
3C153 L	1.2 x 1.1	43	1.6	1166.3	-0.04,0.04,0.07,0.1,0.2,0.4,0.7,1,1.5,2,3,4,7,10,20,40,60,90
3C153 L tap	2.6 x 2.6	49	3.6	1829.4	-0.04,0.04,0.07,0.1,0.2,0.4,0.7,1,2,3,4,7,10,20,40,60,90
3C166 C	0.4 x 0.4	-45	0.4	602.3	-0.03,0.03,0.04,0.07,0.1,0.2,0.4,0.7,1,2,4,7,10,20,40,60,90
3C166 C tap	1.7 x 1.5	72	2.7	615.5	-0.1,0.1,0.2,0.4,0.7,1,2,4,7,10,20,40,60,90
3C166 L	1.3 x 1.3	-16	0.7	436.0	-0.07,0.07,0.1,0.15,0.2,0.3,0.4,0.5,0.6,0.8,1,2,4,7,10,20,40,60,90
3C166 L tap	2.6 x 2.5	71	1.3	454.2	-0.07,0.07,0.1,0.15,0.2,0.3,0.4,0.5,0.6,0.8,1,2,4,7,10,20,40,60,90
3C169.1 C	0.4 x 0.4	60	0.3	8.4	-1,1,1.5,2,4,7,10,20,40,60,90
3C169.1 C lower lobe					-0.6,0.6,0.8,1,1.3,1.6,2,3,4,6,8,10,20,40,60,90
3C169.1 C tap	1.5 x 1.3	67	0.8	14.4	-1.5,1.5,2,3,4,7,10,20,40,60,90
3C169.1 C lower lobe					-1.5,1.5,2,3,4,7,10,20,40,60,90
3C169.1 L	1.5 x 1.4	50	0.4	67.2	-0.2,0.2,0.3,0.4,0.55,0.7,1,1.2,1.6,2,2.4,3,4,7,10,20,40,60,90
3C169.1 L tap	2.6 x 2.4	63	0.6	155.6	-0.15,0.15,0.25,0.4,0.55,0.7,1,1.5,2,2.5,3,4,7,10,20,40,60,90
3C171 C	0.5 x 0.4	63	0.4	181.6	-0.06,0.06,0.075,0.1,0.14,0.2,0.3,0.4,0.6,0.8,1,2,4,7,10,20,40,60,90
3C171 C tap	1.8 x 1.4	78	1.0	315.9	-0.15,0.15,0.2,0.3,0.4,0.7,1,2,4,7,10,20,40,60,90
3C171 L	1.6 x 1.3	59	0.7	828.6	-0.025,0.025,0.04,0.07,0.1,0.15,0.2,0.27,0.32,0.35,0.3,0.4,0.5,0.7,1,2,4,7
3C171 L tap	2.6 x 2.4	60	1.2	978.4	-0.02,0.02,0.04,0.06,0.08,0.1,0.14,0.175,0.2,0.25,0.3,0.4,0.6,0.8,1,2,4,7
OI417 C	0.5 x 0.4	72	0.4	1553.7	
OI417 C tap	1.7 x 1.4	88	0.6	1554.8	
OI417 L	1.6 x 1.3	63	0.5	1945.3	
OI417 L tap	2.6 x 2.4	66	0.7	1946.5	
3C175.1 C	0.5 x 0.4	-55	0.3	100.2	-0.07,0.07,0.1,0.2,0.4,0.7,1,2,4,7,10,20,40,60,90
3C175.1 C tap	1.7 x 1.5	76	1.0	238.1	-0.07,0.07,0.1,0.15,0.2,0.4,0.7,1,2,4,7,10,20,40,60,90
3C175.1 L	1.4 x 1.4	-33	0.6	779.5	-0.02,0.02,0.03,0.04,0.06,0.07,0.1,0.2,0.4,0.7,1,2,4,7,10,20,40,60,90
3C175.1 L tap	2.5 x 2.5	58	1.0	956.2	-0.02,0.02,0.04,0.07,0.1,0.2,0.4,0.7,1,2,4,7,10,20,40,60,90
3C187 C	0.4 x 0.4	38	0.2	3.0	
3C187 C tap	1.5 x 1.3	76	0.4	5.8	-3,3,5,7,10,20,40,60,90
3C187 C upper lobe					-1,1,1.5,2,4,7,10,20,40,60,90
3C187 C core					-0.7,0.7,1,1.2,1.5,2,4,7,10,20,40,60,90
3C187 C lower lobe					-0.7,0.7,0.8,1,1.2,1.5,2,2.5,4,7,10,20,40,60,90
3C187 L	1.6 x 1.3	-6	0.6	19.6	-1,1,1.2,1.5,2,2.5,4,7,10,20,40,60,90
3C187 L tap	2.7 x 2.7	80	1.0	39.0	-0.8,0.8,1,1.2,1.5,2,2.5,3,4,7,10,20,40,60,90
0755+480 C	0.5 x 0.4	49	0.4	5.3	
0755+480 C tap	1.7 x 1.5	65	0.9	-7.4	
0801+364 C	0.5 x 0.4	78	0.3	12.3	-0.7,0.7,1,1.3,2,3,4,7,10,20,40,60,90
0801+364 C tap	1.7 x 1.4	81	0.5	26.9	-0.5,0.5,0.7,0.85,1.3,2,3,4,7,10,20,40,60,90
3C195 C	0.5 x 0.3	-10	0.4	29.8	
3C195 C upper lobe					-0.4,0.4,0.5,0.7,1,1.3,1.7,2,2.5,4,7,10,20,40,60,90
3C195 C core					-0.5,0.5,0.7,1,2,4,7,10,20,40,60,90
3C195 C lower lobe					-0.5,0.5,0.7,1,2,4,7,10,20,40,60,90
3C195 C tap	1.5 x 1.4	83	1.2	74.7	-0.7,0.7,1,2,4,7,10,20,40,60,90
3C195 L	1.8 x 1.2	-12	1.4	250.0	-0.2,0.2,0.3,0.4,0.6,0.8,1,1.5,2,4,7,10,20,40,60,90
3C195 L tap	2.8 x 2.6	-14	2.1	315.2	-0.25,0.25,0.32,0.4,0.5,0.7,1,1.5,2,4,7,10,20,40,60,90
3C196.1 C	0.5 x 0.4	-5.73	0.4	37.6	-0.3,0.3,0.5,0.7,1,1.5,2,4,7,10,20,40,60,90
3C196.1 C tap	1.6 x 1.6	74.07	0.9	146.0	
3C196.1 L	1.6 x 1.3	-6.67	0.6	449.9	-0.03,0.03,0.04,0.07,0.1,0.2,0.4,0.7,1,2,4,7,10,20,40,60,90
3C196.1 L tap	2.7 x 2.6	21.91	1.1	848.5	
3C197.1 C	0.5 x 0.4	47	0.3	7.5	-1,1,1.5,2,2.5,3,4,7,10,20,40,60,90
3C197.1 C tap	1.7 x 1.5	65	1.3	20.9	-1.5,1.5,2,2.5,3,3.5,4,5,6,7,8,10,20,40,60,90
3C197.1 L	1.5 x 1.5	45	1.0	88.1	-0.2,0.2,0.3,0.5,0.7,1,1.5,1.7,2,2.5,3,4,5,7,10,20,40,60,90
3C197.1 L tap	2.3 x 2.3	44	2.0	161.5	-0.3,0.3,0.5,0.7,1,1.5,2,2.5,3,4,7,10,20,40,60,90
4C55.16 C	0.5 x 0.5	46	2.0	5093.2	
4C55.16 C tap	1.7 x 1.5	73	5.3	5348.8	
4C55.16 L	1.1 x 1.1	44	2.1	7868.5	
4C55.16 L tap	2.6 x 2.6	50	3.7	7930.0	
0835+373 C	0.5 x 0.4	85	0.2	135.8	
0835+373 C tap	1.6 x 1.4	90	0.4	147.6	
0850+342 C	0.5 x 0.4	-88	0.2	98.4	-0.06,0.06,0.08,0.1,0.12,0.14,0.2,0.25,0.27,0.4,0.7,1,2,4,7,10,20,40,60,90
0850+342 C tap	1.6 x 1.4	-83	0.3	139.4	-0.045,0.045,0.07,0.085,0.1,0.15,0.2,0.4,0.7,1,2,4,7,10,20,40,60,90
0910+353 C	0.5 x 0.4	-88	0.3		
0910+353 C tap	1.6 x 1.4	-85	0.3		

TABLE 2—*Continued*

Source, Map	Restoring Beam (arcsec)	Position Angle	Noise (mJy)	Peak Flux (mJy)	Levels (percent of peak flux)
3C219 C	0.4 x 0.4	63	0.2	51.3	-0.2,0.2,0.4,0.7,1,2,4,7,10,20,40,60,90
3C219 C lower lobe					-0.1,0.1,0.15,0.2,0.25,0.3,0.4,0.6,0.8,1,2,4,7,10,20,40,60,90
3C219 C tap	1.5 x 1.3	65	0.3	48.3	-0.4,0.4,0.7,1,2,4,7,10,20,40,60,90
3C219 C lower lobe					-0.2,0.2,0.4,0.7,1,1.5,2,3,4,7,10,20,40,60,90
3C219 L	1.5 x 1.4	55	1.7	71.0	-0.7,0.7,0.9,1.1,1.5,2,2.5,3,4,7,10,20,40,60,90
3C219 L tap	2.7 x 2.5	63	4.3	150.8	-0.7,0.7,0.9,1.2,1.5,2,2.5,3,4,7,10,20,40,60,90
3C223 C	0.6 x 0.4	-82	0.5	5.0	
3C223 C tap	1.7 x 1.5	-73	0.8	4.9	
3C234 C	0.6 x 0.4	-80	0.6	62.5	-0.4,0.4,0.7,1,2,4,7,10,20,40,60,90
3C234 C upper lobe					-0.2,0.2,0.3,0.4,0.45,0.55,0.7,1,2,4,7,10,20,40,60,90
3C234 C lower lobe					-0.2,0.2,0.3,0.4,0.55,0.7,1,1.5,2,4,7,10,20,40,60,90
3C234 C tap	1.5 x 1.3	-79	0.8	135.9	-0.2,0.2,0.4,0.7,1,2,4,7,10,20,40,60,90
3C234 L	2.0 x 1.3	-75	2.1	516.6	-0.12,0.12,0.17,0.23,0.3,0.4,0.6,0.8,1,2,4,7,10,20,40,60,90
3C234 L tap	2.8 x 2.3	-78	4.2	861.7	-0.12,0.12,0.14,0.17,0.23,0.3,0.4,0.6,0.8,1,2,4,7,10,20,40,60,90
3C236 C	0.6 x 0.4	-82	0.4	806.2	-0.02,0.02,0.03,0.04,0.07,0.1,0.2,0.4,0.7,1,2,4,7,10,20,40,60,90
3C236 C tap	1.8 x 1.4	-72	1.2	1213.6	
3C236 L	1.8 x 1.3	-84	1.4	2663.5	
3C236 L tap	2.7 x 2.3	-83	2.6	2922.6	
3C244.1 C	0.5 x 0.4	57	0.6	215.6	-0.1,0.1,0.2,0.4,0.7,1,2,4,7,10,20,40,60,90
3C244.1 C upper lobe					-0.07,0.07,0.1,0.15,0.2,0.25,0.4,0.7,1,2,4,7,10,20,40,60,90
3C244.1 C lower lobe					-0.07,0.07,0.1,0.15,0.2,0.25,0.4,0.7,1,2,4,7,10,20,40,60,90
3C244.1 C tap	1.7 x 1.4	72	0.8	345.0	-0.2,0.2,0.4,0.7,1,2,4,7,10,20,40,60,90
3C244.1 L	1.7 x 1.4	54	1.2	1092.4	-0.03,0.03,0.05,0.07,0.1,0.15,0.2,0.3,0.4,0.7,1,2,4,7,10,20,40,60,90
3C244.1 L tap	2.7 x 2.6	50	1.5	1249.8	-0.03,0.03,0.05,0.07,0.1,0.15,0.2,0.4,0.7,1,2,4,7,10,20,40,60,90
3C258 C	0.4 x 0.4	16	0.3	372.4	
3C258 C tap	1.6 x 1.6	63	0.5	383.2	
3C258 L	1.3 x 1.3	-22	0.5	840.6	
3C258 L tap	2.9 x 2.9	47	0.6	846.3	
1125+325 C	0.4 x 0.4	73	0.3	50.0	-0.15,0.15,0.25,0.4,0.7,1,2,4,7,10,20,40,60,90
1125+325 C tap	1.6 x 1.5	-77	0.6	89.4	-0.3,0.3,0.5,0.7,1,2,4,7,10,20,40,60,90
3C263.1 C	0.6 x 0.4	-70	0.3	188.2	-0.05,0.05,0.07,0.1,0.2,0.4,0.7,1,2,4,7,10,20,40,60,90
3C263.1 C tap	1.8 x 1.4	-83	0.7	297.1	-0.05,0.05,0.07,0.1,0.2,0.4,0.7,1,2,4,7,10,20,40,60,90
3C263.1 L	1.7 x 1.4	-68	1.1	1324.3	-0.02,0.02,0.04,0.07,0.1,0.2,0.4,0.7,1,2,4,7,10,20,40,60,90
3C263.1 L tap	2.9 x 2.6	82	4.0	1442.8	-0.1,0.1,0.2,0.4,0.7,1,2,4,7,10,20,40,60,90
3C268.2 C	0.5 x 0.4	84	0.4	13.4	-1,1,2,4,7,10,20,40,60,90
3C268.2 C upper lobe					-0.6,0.6,0.8,1,1.5,2,4,7,10,20,40,60,90
3C268.2 C lower lobe					-0.5,0.5,0.7,1,2,4,7,10,20,40,60,90
3C268.2 C tap	1.6 x 1.4	-85	0.8	23.8	-1.2,1.2,2,4,7,10,20,40,60,90
3C268.2 C upper lobe					-0.7,0.7,1,1.2,1.6,2,4,7,10,20,40,60,90
3C268.2 L	1.6 x 1.2	-85	0.4	87.3	-0.2,0.2,0.3,0.4,0.7,1,1.5,2,4,7,10,20,40,60,90
3C268.2 L tap	2.8 x 2.5	-69	0.9	117.4	-0.3,0.3,0.4,0.6,0.8,1,1.5,2,4,7,10,20,40,60,90
3C268.3 C	0.6 x 0.4	67	0.4	666.1	-0.02,0.02,0.04,0.07,0.1,0.2,0.4,0.7,1,2,4,7,10,20,40,60,90
3C268.3 C tap	1.7 x 1.5	-84	0.6	794.1	
3C268.3 L	1.7 x 1.2	66	2.9	2324.2	-0.04,0.04,0.07,0.1,0.2,0.4,0.7,1,2,4,7,10,20,40,60,90
3C268.3 L tap	2.7 x 2.5	71	4.7	2891.3	
1253+291 C	0.6 x 0.4	-76	0.3	31.9	
1253+291 C tap	1.8 x 1.6	-61	0.4	49.0	
1253+291 L	1.8 x 1.3	-77	0.3	103.4	
1253+291 L tap	2.8 x 2.4	-71	0.5	121.4	
1255+294 C	0.6 x 0.4	-79	0.4	7.1	-2,2,4,7,10,20,40,60,90
1255+294 C tap	1.8 x 1.5	-71	0.5	3.0	
1255+294 L	1.7 x 1.3	-75	0.3	16.5	-0.5,0.5,0.7,1,2,4,5,7,10,20,40,60,90
1255+294 L tap	2.8 x 2.3	-69	0.4	18.8	-0.4,0.4,0.7,1,2,4,5,7,10,20,40,60,90
1256+311 L	1.6 x 1.3	-82	0.3	7.0	-1.2,1.2,1.6,2,3,4,7,10,20,40,60,90
1256+311 L tap	2.7 x 2.5	-65	0.4	6.3	-1.2,1.2,1.6,2,3,4,7,10,20,40,60,90
1256+283 C	0.5 x 0.4	-77	0.3	5.2	
1256+283 C tap	1.7 x 1.5	-64	0.3	1.9	-5,5,7,10,20,40,60,90
1256+283 L	1.6 x 1.3	-79	0.3	20.8	-0.5,0.5,0.7,1,1.5,2,4,7,10,20,40,60,90
1256+283 L tap	2.8 x 2.4	-77	0.7	27.0	-0.7,0.7,1,2,4,7,10,20,40,60,90
3C411 C	0.4 x 0.4	19	1.2	164.8	-0.2,0.2,0.4,0.7,1,2,4,7,10,20,40,60,90
3C411 C tap	1.6 x 1.5	57	0.8	220.4	-0.15,0.15,0.2,0.25,0.3,0.4,0.7,1,2,4,7,10,20,40,60,90
3C411 L	1.4 x 1.2	0	1.2	577.6	-0.07,0.07,0.09,0.12,0.15,0.2,0.25,0.3,0.35,0.45,0.65,1,2,4,7,10,20,40,60,90
3C411 L tap	2.5 x 2.5	52	1.5	698.8	-0.04,0.04,0.07,0.1,0.2,0.3,0.4,0.55,0.7,0.8,0.9,1,1.2,1.5,2,4,7,10,20,40
OW637 C	0.4 x 0.3	-4	1.0	2503.5	
OW637 C tap	1.5 x 1.5	33	1.0	2505.8	
OW637 L	1.4 x 1.1	-11	0.5	2031.6	
OW637 L tap	2.5 x 2.3	-6	0.6	2032.0	
3C427.1 C	0.5 x 0.3	5	0.4	31.5	-0.5,0.5,0.7,1.2,1.6,2,3,5,7,10,20,40,60,90
3C427.1 C tap	1.5 x 1.4	36	0.8	138.3	-0.2,0.2,0.4,0.7,1,2,4,7,10,20,40,60,90

TABLE 2—*Continued*

Source, Map	Restoring Beam (arcsec)	Position Angle	Noise (mJy)	Peak Flux (mJy)	Levels (percent of peak flux)
3C427.1 L	1.7 x 1.1	0	1.4	406.5	-0.1,0.1,0.15,0.2,0.25,0.3,0.5,0.7,1,2,4,7,10,20,40,60,90
3C427.1 L tap	2.8 x 2.3	1	1.9	899.8	-0.1,0.1,0.2,0.3,0.4,0.7,1,2,4,7,10,20,40,60,90
3C435 C	0.4 x 0.4	9	0.5	55.0	-0.3,0.3,0.5,1,2,4,7,10,20,40,60,90
3C435 C tap	1.7 x 1.5	74	0.5	76.9	-0.3,0.3,0.5,0.7,1,2,4,7,10,20,40,60,90
3C435 L	1.4 x 1.3	-4	1.2	225.7	-0.1,0.1,0.15,0.2,0.4,0.7,1,2,4,7,10,20,40,60,90
3C435 L tap	2.6 x 2.6	69	1.7	347.1	-0.1,0.1,0.2,0.3,0.4,0.7,1,2,4,7,10,20,40,60,90
3C441 C	0.4 x 0.4	15	0.4	72.7	-0.23,0.23,0.35,0.5,0.7,1,2,4,7,10,20,40,60,90
3C441 C upper lobe					-0.15,0.15,0.2,0.25,0.3,0.35,0.45,0.65,0.85,1,2,4,7,10,20,40,60,90
3C441 C lower lobe					-0.15,0.15,0.2,0.25,0.3,0.35,0.45,0.65,0.85,1,2,4,7,10,20,40,60,90
3C441 C tap	1.6 x 1.5	66	0.4	128.5	-0.3,0.3,0.6,1,1.5,2,2.5,4,7,10,20,40,60,90
3C441 L	1.3 x 1.1	18	1.5	268.7	-0.15,0.15,0.2,0.23,0.23,0.3,0.4,0.7,1,1.5,2,2.5,3,4,7,10,15,20,30,40,60,90
3C441 L tap	2.4 x 2.4	44	3.0	423.2	-0.1,0.1,0.15,0.2,0.25,0.3,0.37,0.5,0.7,1,1.3,2,4,7,10,20,40,60,90
3C462 C	0.3 x 0.3	41	0.4	45.3	-0.4,0.4,0.55,0.7,0.85,1,1.5,2,3,5,7,10,20,40,60,90
3C462 C upper lobe					-0.3,0.3,0.4,0.5,0.65,0.85,1,1.3,1.7,2,4,7,10,20,40,60,90
3C462 C lower lobe					-0.25,0.25,0.33,0.4,0.5,0.65,0.85,1,1.5,2,3,5,7,10,20,40,60,90
3C462 C tap	1.8 x 1.6	56	0.6	117.5	-0.4,0.4,0.7,1,2,3,5,7,10,20,40,60,90
3C462 L	1.2 x 1.1	33	1.2	166.0	-0.3,0.3,0.4,0.6,0.8,1,2,4,7,10,20,40,60,90
3C462 L icln	2.4 x 2.3	40	3.1	376.4	-0.2,0.2,0.4,0.7,1,2,4,7,10,20,40,60,90
4C45.51 C	0.4 x 0.3	42	1.1	1190.9	-0.02,0.02,0.04,0.07,0.1,0.2,0.4,0.6,1,2,6,10,20,40,60,90
4C45.51 C tap	1.7 x 1.5	64	1.1	1229.5	
4C45.51 L	1.2 x 1.1	38	0.8	1796.7	
4C45.51 L tap	2.6 x 2.6	47	1.2	1936.1	
OZ488 C	0.4 x 0.3	39	0.7	1409.3	
OZ488 C tap	1.7 x 1.5	62	0.9	1409.6	
OZ488 L	1.2 x 1.1	32	0.5	2340.8	
OZ488 L tap	2.5 x 2.4	35	0.7	2341.8	

3C 427.1.—There is complex structure in the lobes in the 6 cm map.

3C 425.—This appears to be two separate double-lobe sources, both with compact hot spots. There is a weak core in the larger source.

3C 462.—Compact hot spots are embedded in the lobe structure.

4C 45.51.—Only the core and faint resolved structure are seen, at 6 cm.

We thank Rogier Windhorst for information on the Westerbork sources, and S. Ryneveld for work on the optical correspondence.

REFERENCES

Gower, A. C., & Hutchings, J. B. 1984, AJ, 89, 1658
Heckman, T. M., van Breugel, W., & Miley, G. K. 1984, ApJ, 286, 509
Hutchings, J. B., Johnson, I., & Pyke, R. 1988a, ApJ, 66, 361
Hutchings, J. B., Neff, S. G., Weadock, J., Roberts, L., Ryneveld, S., & Gower, A. C. 1994, AJ, 107, 471
Hutchings, J. B., Price, R., & Gower, A. C. 1988b, ApJ, 329, 122 (HPG)
Kron, R. G., Koo, D. C., & Windhorst, R. A. 1985, A&A, 146, 38
Neff, S. G., & Hutchings, J. B. 1990, AJ, 100, 1441
Neff, S. G., Hutchings, J. B., & Gower, A. C. 1989, AJ, 97, 1291
Price, R., Gower, A. C., Hutchings, J. B., Talon, S., Duncan, D., & Ross, G. 1993, ApJS, 86, 365